DISSOLVED AND SUSPENDED SEDIMENT TRANSPORT DYNAMICS IN TWO AGRICULTURALLY DOMINATED WATERSHEDS, MCLEAN COUNTY, ILLINOIS

Laura A. Hanna

88 Pages August 2013

This thesis investigates the sediment transport dynamics during baseflow and storm flow conditions in the main tributaries of the two drinking water reservoirs in McLean County, Illinois.

DISSOLVED AND SUSPENDED SEDIMENT TRANSPORT DYNAMICS IN TWO AGRICULTURALLY DOMINATED WATERSHEDS, MCLEAN COUNTY, ILLINOIS

Laura A. Hanna

88 Pages August 2013

Protecting drinking water resources is important to the economic, social, and environmental quality of the Midwestern United States. Increased sediment levels can lead to degraded water quality, reduced aquatic biodiversity, impeded recreational usage, and reduced reservoir volume. In this study I investigated the sediment transport dynamics in the main tributaries of two drinking water reservoirs in McLean County, Illinois. The two watersheds have similar hydrology, climate, and land-use, where over 80% of the land cover is agriculture, but there is a significant difference in watershed size and stream gradient. Using suspended sediment concentrations and field discharge measurements during baseflow and storm flow conditions, the suspended sediment and nutrient loads were generated for each sub-watershed over for the duration of the study period.

Because of different watershed characteristics, the sub-watersheds responded differently to precipitation events throughout the study period as seen by the varying discharge, total suspended sediment loads and nutrient loads. During baseflow conditions, Six Mile Creek (SMC) transported more total suspended sediment per drainage area than Money Creek (MC). However, storm flow transported 99.76% of the suspended sediment on SMC and 92.56% of the

sediment on MC. MC had a stream baseflow and storm discharge (Q) that was twice as high as SMC and had sediment loads that were one to four times larger than SMC because of the larger sub-watershed drainage area of MC. Total suspended sediment (TSS) loads were seen with increasing Q and peaked in the springtime on both streams during storm events. The TSS-Q relationships were dynamic on both streams and impacted by sediment availability, precipitation, and in-channel processes like lateral bank migration, streambank erosion, and external soil erosion. SMC transported almost twice the amount of nitrate as nitrogen and chloride load compared to MC. Nutrient transportation occurred entirely during storm events on both streams.

DISSOLVED AND SUSPENDED SEDIMENT TRANSPORT DYNAMICS IN TWO AGRICULTURALLY DOMINATED WATERSHEDS, MCLEAN COUNTY, ILLINOIS

LAURA A. HANNA

A Thesis Submitted in Partial
Fulfillment of the Requirements
for the Degree of

MASTER OF SCIENCE

Department of Geography-Geology

ILLINOIS STATE UNIVERSITY

2013

DISSOLVED AND SUSPENDED SEDIMENT TRANSPORT DYNAMICS IN TWO AGRICULTURALLY DOMINATED WATERSHEDS, MCLEAN COUNTY, ILLINOIS

LAURA A. HANNA

THESIS APPROVED:

_______________	______________________
Date	Eric W. Peterson, Chair
_______________	______________________
Date	Catherine C. O'Reilly
_______________	______________________
Date	Lisa Tranel

ACKNOWLEDGMENTS

I would like to thank my committee, Drs. Eric Peterson, Catherine O'Reilly, and Lisa Tranel for their guidance, knowledge, support, and time throughout my graduate studies and my thesis project. I would like to thank the City of Bloomington who funded my thesis research. I would also like to thank Jill Mayes, Tony Alwood, and Rick Twait from the City of Bloomington for their field and technical support. I would like to thank Dr. Robert (Skip) Nelson for the opportunity to work with EarthScope and for providing me the most enjoyable Graduate Assistantship I could have asked for. I thank my undergraduate field and lab assistants, Laura Sugano and Evan Meinzer. Lastly, I thank all of my friends and family for their support and encouragement during my time at Illinois State University.

L. A. H.

CONTENTS

TABLES

FIGURES

Figure Page

CHAPTER I

INTRODUCTION

Literature Review

World-wide sediment transport to downstream rivers, lakes, and reservoirs poses a threat to the human and ecological environment. Increased sediment levels degrade water quality, reduce aquatic biodiversity, impede recreational usage, and reduce reservoir volume and lifetime (Huenemann et al, 2012, Graf et al., 2010). Land use and climatic patterns influence the rate, timing, amount, and composition of sediment transport.

There are a range of factors that control sediment transport in water: slope, morphology, soil texture, climate, temperature, and land use (Salant et al., 2008; Pelletier, 2012). Low-gradient streams mobilize the streambed more frequently than higher-gradient stream systems as a result of finer substrate (Peterson et al., 2008). In areas of similar relief, suspended sediment increases linearly with rainfall/runoff (Ludwig and Probst, 1998, Restrepo et al., 2006, Pelletier, 2012). Sediment can be derived from internal and external sources like bank erosion or debris flows (Salant et al., 2008). Soil texture influences suspended sediment as soil composed of mostly silt will be more easily eroded than a soil of sand and gravel (Pelletier, 2012). Areas with high mean temperatures can contain more finely textured soil leading to more suspended sediment transport as chemical weathering rates increase with increasing temperature (Pelletier, 2012).

Land use can have a strong influence on suspended sediment transport. Human induced land use changes associated with agriculture, deforestation, and urbanization have significantly increased runoff, sediment yields, and erosion in streams (Trimble, 1999, Vache et al., 2002). In 2000, the U.S.EPA identified agriculture as the leading source of impairment from sediment to rivers in the U.S. (US.EPA, 2000). In the Midwestern US, total suspended sediment was significantly higher in agriculture watersheds compared to urban watersheds during baseflow, while total suspended sediment was similar during storm flow (Miller et al, 2011). For the Midwestern United States, the agricultural industry poses the greatest threat to increased sediment delivered to downstream rivers, lakes, and reservoirs (Graf et al., 2010, U.S.EPA, 2000). Monitoring during a variety of weather conditions and different times of the year can help determine when suspended sediment is being transported.

Suspended sediment concentrations are directly related to discharge (Salant et al., 2008). Most sediment entering a reservoir is being transported during storm events, when stream discharge is high (Gao and Josefson, 2012; Fraley et al., 2009). Sediment supply is usually greatest during the early period of a storm event, as readily available sediment sources from inside the channel are mobilized and transported (Williams, 1989). In addition to storm based events, there are diurnal variations where suspended sediment increases by three to four times in the evening, likely from bioturbation from microorganisms and aquatic life (Gillian, 2005, Loperfido et al., 2010). Seasonally, sediment delivery has been observed to peak in the spring months when discharge was high (Salant et al. 2008).

The transport of suspended sediment is influenced by water availability. Droughts are one of the most devastating natural disasters in the United States, impacting the environment, economy, and society (Allen et al., 2011). Droughts negatively impact the water supply, water quality, crop and rangeland production, power generation, and recreational activities

(Woodhouse & Overpeck, 1998). There is potential for higher sediment transport when there is a storm event during a drought making seasonal and annual field collection important (Allen et al., 2011). Monitoring of drought conditions and sediment transport has shown that infrequent storm events during drought generate greater river sediment input than similar magnitude events under average moisture conditions (Heritage and Van Niekerk, 1995). During drought, there can be a build-up of available sediment to be transported and when a storm occurs, there are often elevated levels of sediment able to be transported. However, overall less sediment is likely to be transported through the system due to the reduced quantity of flow (Heritage and Van Niekerk, 1995). As sediment transport and delivery is a dynamic process, it is important to study how short term changes impact the hydrologic system.

Suspended sediment increases turbidity, negatively impacting aquatic ecosystems. Turbidity is a measure of the ability of water to transmit light and is directly correlated to the amount of material suspended in the water column; the more material in suspension, the higher the turbidity. Turbidity interferes with communication signals, which can alter predator-prey interactions and alter mate choices (Graf et al., 2010, Huenemann et al, 2012). As turbidity increases and light transmittance decreases, the visual acuity of predators like the largemouth bass (*Micropterus salmoides*) and yellow perch (*Perca flavescens*) is reduced, decreasing the efficiency of fish to forage and feed (Huenemann et al., 2012). Elevated suspended sediment concentrations can cause a decrease in specific growth rate (percent change in mass per day) at all life stages of the whitetail shiner, (*Cyprinella galactura*) and federally threatened spotfin chub, (*Erimonax monachus*) (Sutherland & Meyer, 2007). Elevated suspended sediment (100-500 mg/L) also reduced the respiratory success of the whitetail shiner and spotfin chub as the fish gills became clogged from high sediment (Sutherland & Meyer, 2007). A decline in aquatic populations can become a public concern if recreational activities become impeded.

Suspended sediment can reduce reservoir storage capacity. Worldwide, reservoir storage loss from sedimentation ranges from 0.42% per year in Algeria (Khanchoul et al., 2012) to 3.03% in Ethiopia (Haregeweyn et al., 2012). The annual loss of reservoir capacity in the United States is greater than 2% on the west coast, decreasing to 0.81-1.2% in the Midwest, and is less than 0.4% on the east coast (Graf et al., 2010, Ackerman et al., 2009). Illinois reservoirs have an annual reservoir loss of 0.81-1.2% from sedimentation (Ackerman et al., 2009). The typical rate of reservoir sediment input ranges broadly within a stream system, often with short periods of rapid change (Graf et al., 2010).

The temporal pattern that develops between stream discharge (Q) and total suspended sediment (TSS) during a storm is called hysteresis. The resulting Q-TSS hysteresis patterns explain time-varying sediment support and transport, duration, and flow response. At low Q, fine deposited sediment are entrained (Hudson, 2003) or from bank material that has already collapsed (Lenzi and Lorenzo, 2000). At higher Q, more coarse sediment is able to be entrained, and can be an increase of bank and channel hydrological erosion, and sediment contribution from external sources like surface soil erosion (Lefrancois et al., 2007). There are two general patterns of hysteresis that compare TSS and discharge, with clockwise and anti-clockwise patterns being the most frequent (Figure 1). A clockwise hysteresis loop is when the TSS peak arrives before the Q peak. A clockwise loop infers that the sediment mobility is restricted during the event for the specific range of Q (Lefrancois et al., 2007). Remobilization of in-channel fine sediment particles causes entrainment. Often, particle production by erosion during a storm event is not able to resupply the decrease in sediment. Anti-clockwise hysteresis occurs when the TSS peaks after the peak Q. This is understood to be caused by an increase/arrival of distant particles from upstream (Lefrancois et al., 2007) or from a new sediment source that collapsed, for example in a cutbank. These patterns can vary depending on flow and sediment availability, generating double clockwise or anti-clockwise patterns that are seen in streams when there are two peaks in Q.

(a)

(b)

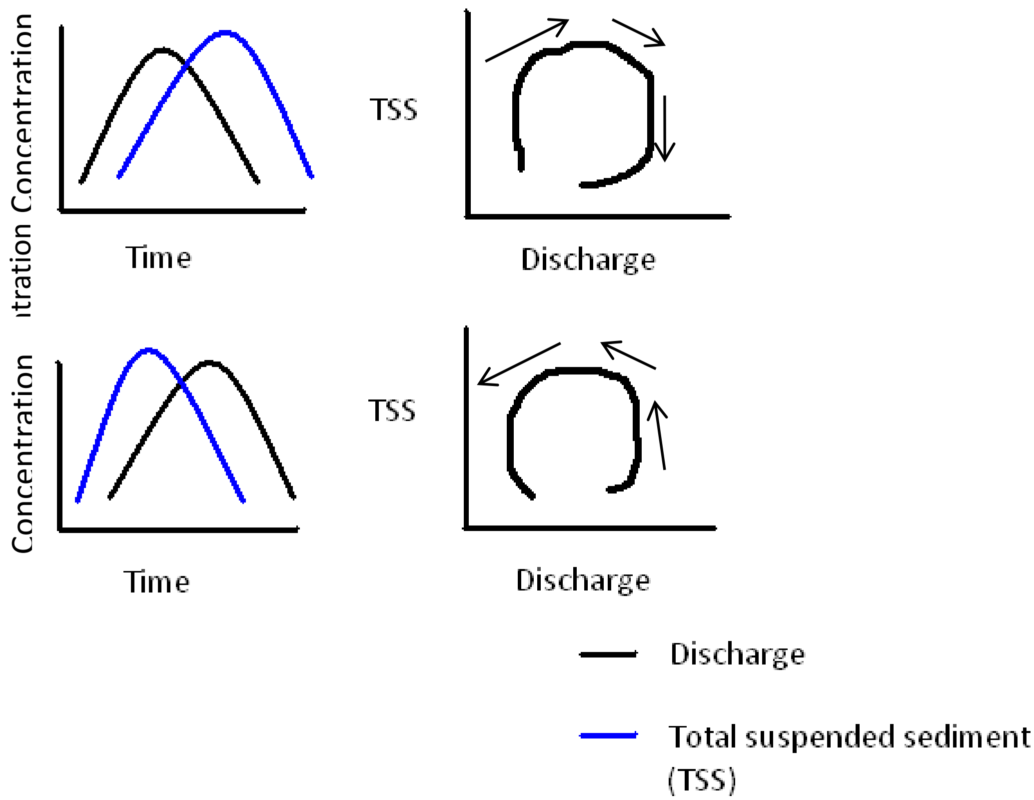

Figure 1: General hysteresis patterns indicating (a) clockwise hysteresis pattern and (b) anti-clockwise hysteresis pattern. The black arrows indicate the direction of total suspended sediment (TSS) concentration movement over time.

Nutrient concentrations are often correlated to land use type, discharge, and suspended sediment. Worldwide, Alvarez-Cobelas et al. (2008) found catchments dominated by agriculture land use had four times more total nitrogen than catchments dominated by forest and two times more total nitrogen than catchments dominated by pasture. Excess nutrients from fertilizers not used by the crops can leach into the groundwater and enter the nearby stream (Miller et al, 2011). As a result of high nitrogen levels, many municipal drinking water reservoirs frequently exceed the EPA maximum contamination level (MCL), 10 mg/L nitrate as nitrogen (NO_3-N) or 45 mg/L nitrate (NO^{-3}) (US.EPA, 1998, Miller et al, 2011). From 1986-2003, Lake

Bloomington (IL), one of the reservoirs in this study, consistently exceeded the EPA MCL nitrate levels (Kovacic et al., 2006). A primary concern of elevated nitrate is the risk of methemoglobinemia (blue baby syndrome), which causes neural damage in infants 6 months old or younger (Borah et al., 2003). Excessive nitrate increases algal production, leading to eutrophic conditions and to an increase in fish mortality (Graf et al., 2010). Nitrate occurs naturally in soil, forming from nitrification and from microorganisms breaking down fertilizers, plants, and manures (Eby, 2004). Storm events transport a large portion of excess nutrients and sediment (Drewry et al., 2009). Nutrients can bind to sediment in transport, which can contribute significant nutrient pollution to receiving streams (Miller et al., 2011). This study will focus on NO3-N as it is a strong proxy for total nitrogen and is generally the most dominant nitrogen species (Van der Hoven et al., 2008).

Solute concentrations change with changes in flow. Chloride concentrations have been seen to be elevated in pre-storm event waters (Kennedy et al., 2012). Chloride is a concern to water quality as road salt is a constant source during the winter months within both watersheds. Winter months are also not the sole period of elevated chloride concentrations, summer storms can flush residual chloride from the unsaturated zone into stream baseflow (Lax and Peterson, 2009). Chloride concentrations have been seen to increase with increasing tile drainage (Skaggs et al., 1994). Nitrate as nitrogen and chloride concentrations will be assessed during baseflow and storm flow conditions and seasonal variations determined.

Study Sites

The two study watersheds, Lake Bloomington and Evergreen Lake, are located in central Illinois in McLean County (Figure 2). Lake Bloomington was constructed in 1929 and Evergreen Lake in 1971 to serve as drinking water reservoirs for the City of Bloomington (Evergreen Lake

Watershed Management Plan, 2008). Lake Bloomington study catchment (180 kilometer^2/ 69.5 mile^2) and Evergreen Lake (106.49 kilometer^2/ 41.1 mile^2) are both upland headwater catchments of the Mackinaw River (Table 1). The study site on Six Mile Creek (SMC), which is part of the Evergreen watershed, is just over 0.8 km (0.5 mile) upstream from the reservoir, while the site on Money Creek (MC) within the Bloomington watershed is just over 3.2 km (2 miles) upstream. The monitored sub-catchments on Evergreen Lake (47.27 kilometer^2/ 18.25 mile^2) and on Lake Bloomington (112.56 kilometer^2/ 43.46 mile^2) are adjacent to one another (Figure 2). The drainage area of Lake Bloomington is almost 70% larger than the size of Evergreen watershed, but has less than half the storage capacity compared to Evergreen Lake (Table 1). Lake Bloomington also has a smaller lake surface area, so the drainage to surface area ratio for Lake Bloomington is 68:1, while Evergreen is 29:1. Both reservoirs have been modified during their use to increase the storage capacity. Lake Bloomington originally had a storage capacity of 9,103,096 m^3 (7,380 acre-feet). A bathymetric map was created from a sedimentation survey conducted in 1999 by Hanson Engineering, and determined that Lake Bloomington had a storage capacity of 8,348,205 m^3 (6,768 acre-feet) (Lake Bloomington Watershed Management Plan, 2008). The storage capacity of Lake Bloomington decreased 754,891 m^3 (612 acre-feet) over 70 years. There was no previous bathymetric mapping of Evergreen Lake, but the original storage capacity was 19,095,299 m^3 (15,480 acre-feet) (Evergreen Lake Watershed Management, 2008) (Table 1).

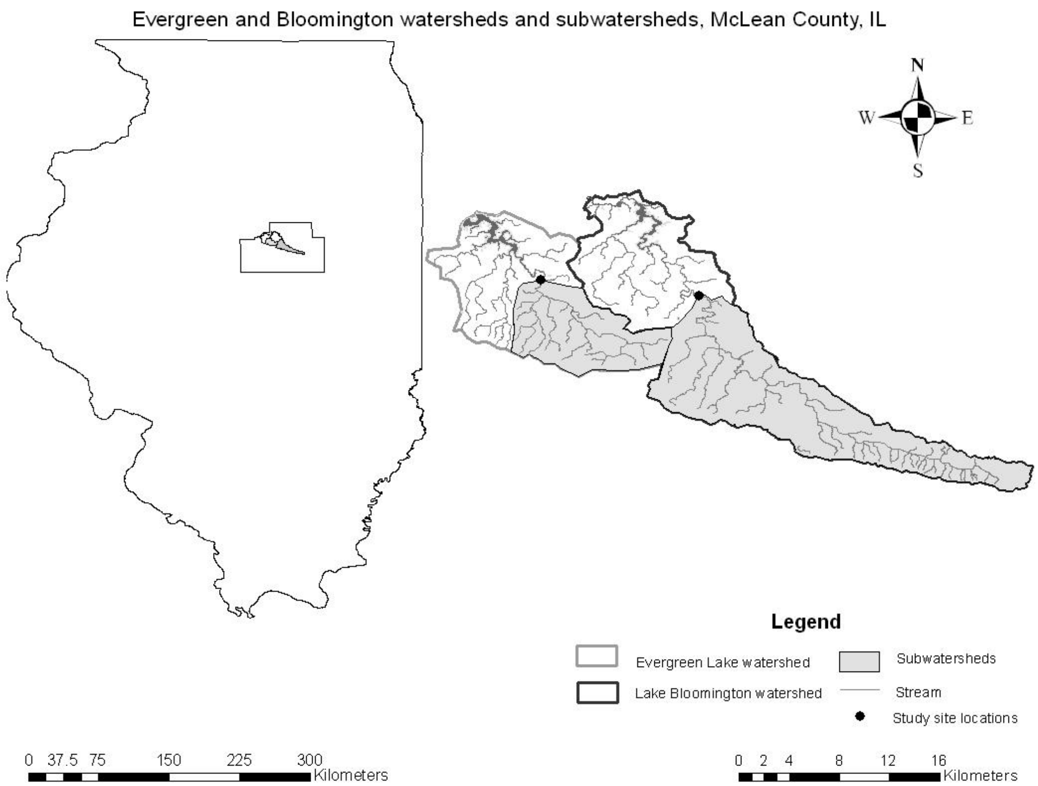

Figure 2: Evergreen and Bloomington watersheds and sub-watersheds delineated with research site locations, McLean County, IL.

Table 1: Watershed characteristics of Lake Bloomington and Evergreen Lake, McLean County, IL (Evergreen Lake Watershed Management Plan, 2008, Lake Bloomington Watershed Management Plan, 2008).

Location	Watershed size		Sub-watershed size		Stream gradient		Sediment delivered by erosion from		Reservoir storage capcity	
	km²	mi²	km²	mi²	m/km	ft/mi	kg	ton	m³	acre-ft
Lake Bloomington	180	69.5	112.56	43.45	0.77	4.06	$1.14x10^6$	$1.26x10^3$	$9.1x10^6$	$6.77x10^3$
Evergreen Lake	106	41.1	47.27	18.25	1.34	7.8	$1.94x10^6$	$2.14x10^3$	$1.91x10^7$	$1.55x10^4$

Both watersheds are dominated by row crop agriculture. Both sub-watersheds are dominated by agriculture as well (Figure 3). The Soil and Water Conservation District (2008) estimates that 30.35 km² (7,500 acres) in both watersheds are tiled, 18% of Lake Bloomington and 25% of Evergreen. Presently, Evergreen Lake has at least 3.1 km² (758 acres) of the total

104.13 km² (25,730 acres) under different conservation practices and no homes directly surrounding the lake (Evergreen Lake Watershed Management Plan, 2005). The Lake Bloomington watershed has 0.86 km² (213 acres) of filter strips that were installed and is surrounded by residential homes (Lake Bloomington Watershed Management Plan, 2008).

Historical Context

Previous work concluded the sediment delivery to Lake Bloomington from MC was significantly less than that found in Evergreen Lake from SMC in 2005 (Lake Bloomington Watershed Management Plan, 2008). In 2005, the City of Bloomington surveyed both riverine systems and determined that Lake Bloomington had 1,143,053 kg (1,260 tons) of sediment delivered annually in comparison to 1,936,839 kg (2,135 tons) of sediment supplied to Evergreen Lake using a Rapid Assessment, Point Method (RAP-M) (Table 1) (Evergreen Lake Watershed Management Plan, 2008, Lake Bloomington Watershed Management, 2008). The total sediment delivered annually to Lake Bloomington was estimated at 17,236.5 kg (19 tons) per square mile of drainage area; while 48,080.8 kg (53 tons) per square mile of sediment was delivered annually to Evergreen Lake (Kinney, 2005). This difference was probably due to a more stable channel and lower stream gradient on MC compared and more incised river channels on SMC (Kinney, 2006).

Historical TSS data was available from the City of Bloomington Water Purification plant for both sites from January 2005-April 2012 (Figure 4a and 4b). The historical data for both streams ranged in TSS concentration from 2-1000 mg/L.

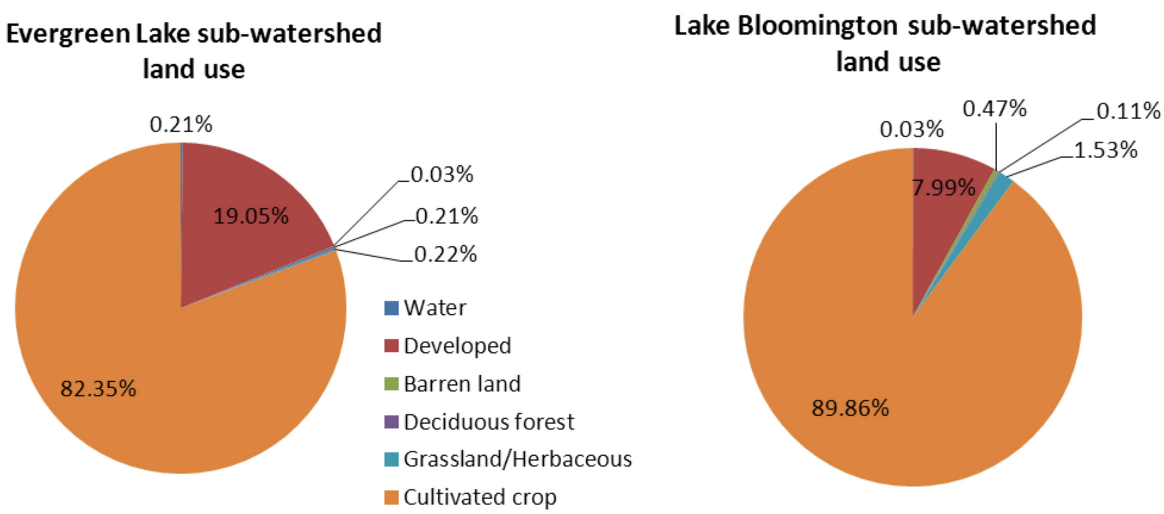

Figure 3: Land use of the sub-watersheds on Six Mile Creek in the Evergreen Lake watershed and Money Creek in the Lake Bloomington watershed, McLean County, IL.

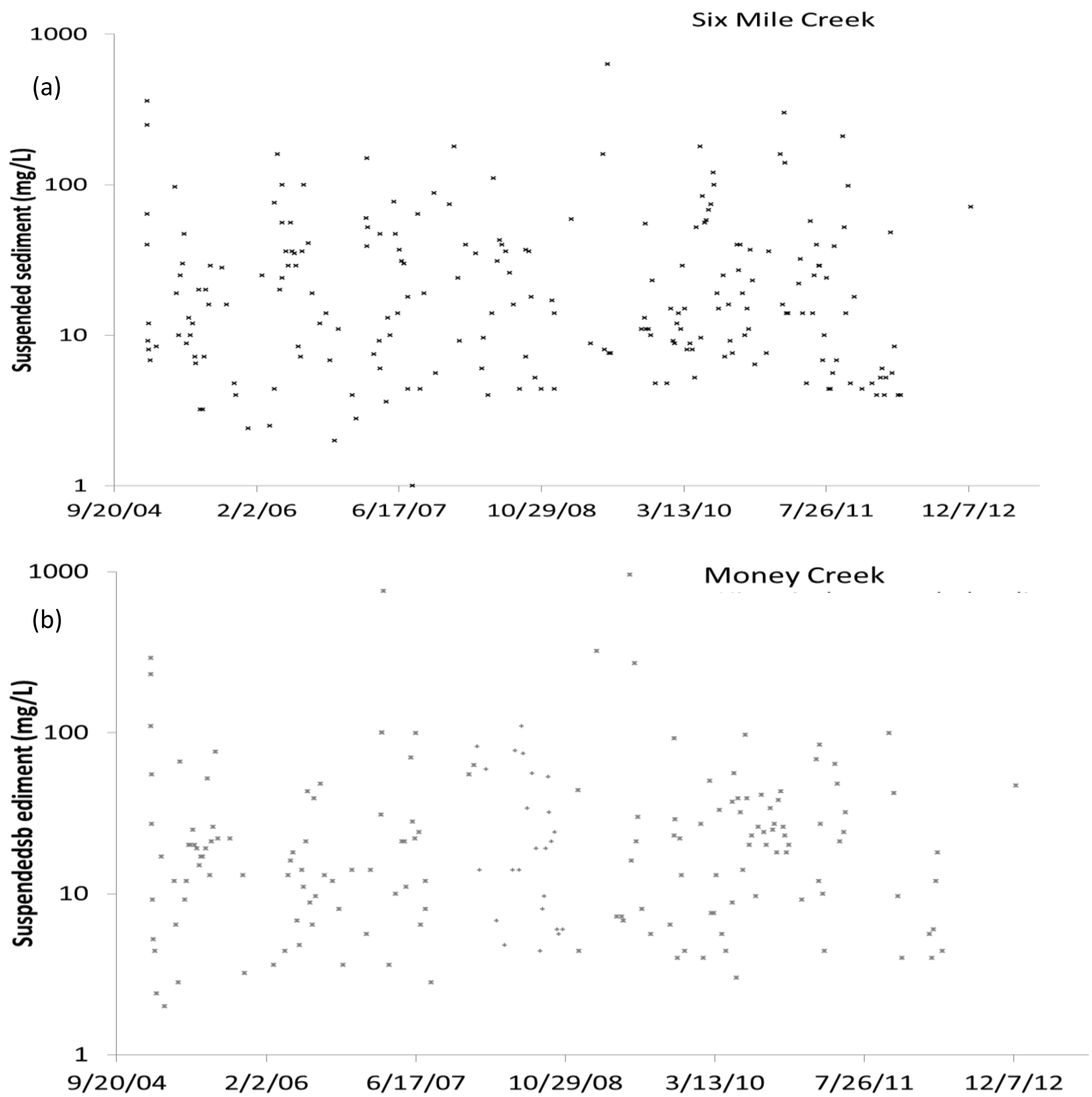

Figure 4: Historical suspended sediment data (September 2004-July 2012) on (a) SMC and (b) MC.

Geology

The geological history of McLean County, Illinois is dominated by multiple glacial advances. The last glaciation was the Wisconsinan period, which ended 12,000 years ago. The glaciation formed a series of moraines across east-central and northeastern Illinois. Just west of Evergreen Lake is the Bloomington end moraine, which caused the land adjacent to Evergreen Lake to have a slightly steeper slope than Lake Bloomington (Evergreen Lake Watershed

Management Plan, 2008). The Bloomington moraine lies just south of Lake Bloomington (Lake Bloomington Watershed Management Plan, 2008). The El Paso Moraine lies to the northeast of Evergreen Lake.

The glacial movement, running water, and windblown deposits have contributed to the formation of the landscape within McLean County, IL. The land north of the Bloomington Moraine is gently sloping (1-4% slope), except for steeper slopes (4-10%) near the Mackinaw River to the north of the watershed (Lake Bloomington Watershed Management Plan, 2008). Both watersheds lay within the Till Plains Section of the Central Lowland Province physiographic area. Both are located in the Bloomington Ridged Plain, which is a rolling low-relief landscape. Overall, the soils are mostly silt loams and silty clay loams, poorly drained, and are very fertile, with high organic content and high resistance to drought (Soil Survey of Mclean County, 2002). The most common soil type in both watersheds is Sable silty clay loam, which is a by-product of the windblown silt, loess, which was distributed during the glacier retreat (Evergreen Lake Watershed Plan, 2008). This soil has slow infiltration rates as there is high clay content causing poor drainage with high runoff levels. The second most common soil is Ipava silt loam, which occurs on landscapes with a slope of 0 – 2 percent and is poorly draining (Soil Survey of McLean County, 2002).

Statement of Purpose

The objective of this research was to expand on aspects of previous studies conducted by Kinney (2005 & 2006) to further understand the sediment transport and nutrient concentrations dynamics to help manage the water resources of McLean County, IL. The previous work was conducted during a shorter time frame and did not incorporate any seasonal or storm monitoring. This project analyzed suspended sediment dynamics in two adjacent watersheds that differ in stream gradient and watershed size in McLean County, IL. Suspended sediment loads and water quality characterization were assessed for both SMC and MC during a yearlong study (July 2012-March 2013). Discharge was monitored during baseflow and storm event conditions to provide an index for the amount of suspended sediment able to be transported using a sediment rating curve. This project was accomplished by comparing suspended sediment, discharge, and nutrient compositions.

The overarching question was:

- ❖ What is the rate of suspended and dissolved sediment transport in the Lake Evergreen watershed and the Bloomington Lake watershed during a drought year?

Below are four hypotheses that are addressed to answer the above question:

1. Will similar discharges produce different sediment transport loads between the two watersheds?

Reasoning: It was hypothesized that sediment loads will increase with discharge. Given the greater slope system and more actively incising channel in Lake Evergreen, it was predicted SMC will generate a larger sediment load than MC.

2. Is baseflow suspended sediment transport the same amount in both watersheds?

Reasoning: SMC in the Lake Evergreen watershed would have a higher suspended sediment concentration leading to a higher suspended sediment load than MC in the Bloomington Lake watershed as Kinney (2005) showed that Evergreen Lake receives twice the amount of sediment than Lake Bloomington. SMC also has a 48% higher stream gradient and a more actively incising river channel than MC, which may also be a factor (Kinney, 2006).

3. Is the suspended sediment transported during an event flow the same in both watersheds?

Reasoning: I hypothesized that suspended sediment would increase with increasing discharge and as MC has a larger watershed area, MC would have a higher Q and also a higher suspended sediment load during storm events.

4. Are the anion concentrations and loads the same in both watersheds?

Reasoning: MC would have higher nutrient levels than SMC as MC is a larger watershed. It was hypothesized that nitrate would peak in the spring and chloride would peak in the winter on both streams when seasonal variations were taken into account.

CHAPTER II

METHODS

Instrumentation Set-up

Each stream site had an automated water sampler (Sigma 900Max) installed to measure and collect water samples that were analyzed for suspended sediment and nutrient concentrations. Each sampler contained 24 1-L bottles. The Sigma 900Max logged the water depth and velocity continuously every 15 minutes, which were recorded internally in the automatic collector's memory (HACH manual). The velocity was recorded using an average area velocity probe, which was submerged, sitting just off the bottom of the stream bed close to the thalweg of the stream. The velocity probe had a minimum reading of 0.06 m/s (0.2 ft/s) and would not record any velocity below 0.06 m/s (0.2 ft/s) (HACH manual). The logged data were retrieved every two weeks in the field using a DTU II. The logged data (velocity, depth, time, and flow) were transferred to the Insight computer program for analysis back in the lab.

Suspended Sediment

Every two weeks, grab samples were collected over the edge of the bridge with a 1-L bottle attached to a clamp using a string to lower the container to the stream midpoint. Grab samples were collected from the same location every time and each bottle was rinsed three times before a sample was collected. The stream name, date, and time of collection were recorded on the container, and bottles were stored at 4 °C. A portable, HACH 2100Q turbidity meter was used in the field to determine turbidity during each site visit. A Sigma 900Max sampler was used to collect storm flow samples. The instrumentation was activated to collect water samples during storm events when the water level thresholds increased 7.62 cm (3 inches) above baseflow, which was measured by the attached pressure transducer, (range 0 to 9 meters), with an accuracy of ±0.018 m. Ideally, the water threshold trigger would have been higher but due to the drought conditions, the threshold was reduced to be able to collect storm events. The threshold changed throughout the study period, using the previous two weeks of stage data to assess what the trigger level would be adjusted to. The trigger level threshold ranged from roughly 0.9 feet to 1.7 feet at the highest on both SMC and MC. When the threshold was reached, the sampling program immediately began sampling. The Sigma 900Max collected a total of 24 samples for each storm event. The sampling intervals were standardized (Appendix A), but depending on the size of the storm the sampling intervals were subject to change (Outeiro et al., 2010). After each sample collection of the event flow water samples, sample bottles were replaced and brought to the Department of Geography-Geology, Illinois State University laboratory in Normal, IL for suspended sediment and nutrient analysis.

To determine the total suspended sediment concentration (TSS), each sample was agitated by shaking the 1L bottle for at least 10 seconds and a known volume (roughly 800 ml) was measured with a graduated flask. The known volume of sample was filtered using glass microfiber filters (Whatman 934-AH, diameter 27mm, particle retention of 1.5 µm) that were pre-combusted at 540°C in a muffle furnace for six hours. Each filter with sediment was dried at 105 °C for 24 hours in a drying oven. The dried weight was measured after cooling. The TSS was found using:

$$TSS\ \frac{mg}{L} = \frac{(mass\ of\ filter + dried\ sediment\ (g\ ) -\ mass\ of\ filter\ \ g}{sample\ volume\ of\ water\ \ ml}\ x\frac{1000\ ml}{1\ L}x\ \frac{1000\ mg}{1\ g} \qquad \text{Eqn.1}$$

The loss-on-ignition method (ASTM, 2000) was used to determine the organic and inorganic suspended sediment (Eqn.2 & 3).

Organic suspended sediment (mg/L) =

$$\frac{\text{weight of sediment +filter before ignition (g)} - \text{weight of residue+filter after ignition (g)}}{sample\ volume\ \ ml} \; x \frac{1000\ ml}{1\ L} \; x \frac{1000\ mg}{1\ g}$$

Eqn. 2

Inorganic suspended sediment (mg/L) =

$$\frac{\text{weight of residue+filter after ignition} \ \ g\ - \text{weight of filter(g)}}{sample\ volume\ \ ml} \; x \frac{1000\ ml}{1\ L} x \frac{1000\ mg}{1\ g}$$

Eqn. 3

Discharge

Discharge (Q) was measured using the velocity-area method (Mosely and McKerchar, 1993). Baseflow velocity was determined using a handheld, Sontek Flowtracker Acoustic Doppler velocimeter (ADV), velocity range – 0.001 m/s (0.003 ft. /s) to 4.5 m/s (15 ft. /s) (FlowTracker Manual), using the mid-section method (Eby, 2004). During baseflow conditions, velocity was measured at 0.6 the distance from the water surface to streambed. Discharge was determined every two weeks when grab samples were collected.

Storm Flow

During storm events, a bridge board was used to lower all sampling equipment into the stream over the edge of the bridge. A Sigma portable velocity meter, minimum velocity reading of 0.03 m/s (0.01 fps) (Sigma Manual), secured on top of 6.8 kg weight was lowered into the stream. During storm events, when flow exceeded 1.07 m (3.5 ft) the average velocity was calculated from an average velocity between 0.2 and 0.8 the depth of the water. The stream length was initially measured and divided into three equal widths and velocity measurements were recorded to determine if there was a rapid change in stage during the storm event. If the stage was not rapidly increasing, further velocity measurements were taken along the transect.

The three initial velocity measurements were repeated at the end to make sure velocity and depth measurements were consistent.

Suspended Sediment Load

Suspended sediment loads for each period of baseflow and storm flow were calculated. The loads were determined by multiplying the parameter (mg/L) by the water discharge (m^3/s) by a factor of 1000 to convert the load to mg/s. Total baseflow load was calculated by Eqn. 4, taking the average baseflow load multiplied by the difference in time multiplied by two conversion factors and summed to calculate the total baseflow load in kilograms.

$$Total\ baseflow\ load\ \ kilogram\ =$$

$$\sum_{i=1}^{n} Avg\ baseflow\ load\ (\frac{mg}{s}) x\ \ Time_{i+1}\ \ min\ \ - Time_{i}\ \ min\ \ \ x\ \frac{60\ sec}{1\ min} x \frac{1\ g}{1000\ mg} x \frac{0.001\ kg}{1\ g}$$

Eqn. 4

Suspended sediment load with respect to the change in time between the samples were determined for each storm event. The total suspended sediment load was determined by adding the parameter load per time period (mg/s) with the previous, dividing by two to find the average and multiplying by the change in time and then took the summation from all storm events to find the total suspended sediment load, determined by the equation 5.

$$Total\ storm\ load\ \ \ kg\ =$$

$$\sum_{i=1}^{n} \frac{L_{i+1}\ \frac{mg}{s} + L_{i}\ \frac{mg}{s}}{2}\ \ x\ T_{i+1}\ \ min\ \ - T_{i}\ \ min\ \ \ x\ \frac{60\ sec}{1\ min} x \frac{1\ g}{1000\ mg}\ x \frac{0.001\ kg}{1\ g}$$

Eqn. 5

The percentage baseflow and storm flow were determined by dividing the total baseflow or storm flow by the total load and multiplying by 100.

Reservoir Accumulation

Rough estimates of how much of the TSS load per stream was ending up in the reservoirs were calculated. The total TSS load per stream was multiplied by a conversion factor to convert kilograms to grams, multiplied by the density of silicate sediment particles (2.65 g/cm³) and divided by another conversion factor to find the load accumulated by year in cubic meters (Eqn. 6.) The reservoir volume was then divided by the TSS load/year to find the number of years required for TSS to fill in the reservoir (Eqn. 7).

$$\text{TSS load (kg/year)} * \frac{1000\ g}{1\ kg} * \frac{1\ g}{2.3\ \frac{g}{cm^3}} * \frac{1 cm^3}{1{,}000{,}000 m^3} = \text{TSS volume } (m^3/\text{year}) \qquad \text{Eqn. 6}$$

$$\frac{Reservoir\ volume\ (m^3)}{TSS\ volume\ (m^3/\text{year})} = \#\ of\ \ years\ for\ reservoir\ to\ fill\ in$$

Eqn. 7

Nutrients

Nutrient concentrations (mg/L) for nitrate as nitrogen and chloride were analyzed on a Dionex IC 1100 ion chromatograph. A 60 ml water samples for nutrient analysis was filtered in the field with syringe and glass fiber filter (Millipore Grade A-E, pore size 1 µm, diameter 25mm). Baseflow and storm event water samples were analyzed for nutrient concentrations. Nutrient concentrations were used to assess water quality by comparing the water to the EPA drinking water standards. Drinking water standards for the following anions should be below; chloride – 250 mg/L, and nitrate as nitrogen – 10.0 mg/L (US.EPA, 2009). Duplicates and blank samples were run for every ten samples to ensure quality control and quality assurance. The summer, autumn, and winter months were compared for nutrient concentrations and loads based on the traditional changing of solstice and equinox. Nutrient loads for nitrate as nitrogen and chloride baseflow and storm flow were calculated using the same equations as suspended sediment (Equations 4 and 5).

CHAPTER III

RESULTS

Overview

The study period was July 12, 2012-March 28, 2013. There were 10 baseflow measurements collected on SMC and nine on MC. There were 16 storm discharge measurements on SMC and 14 storm discharge measurements on MC. There were 12 storm events captured on SMC and eight on MC. Nutrient data for nitrate and chloride were determined for the baseflow and storm discharge measurements on SMC and MC. Unless noted, statistical differences were not significant.

Weather

During the study period, central Illinois experienced a range of weather conditions. The beginning of 2012 started as a drought year. At the end of August 2012 the remnants of Hurricane Isaac came through and reduced the drought conditions from extreme to severe (ISGS, 2012) (Table 5a). In 2012, total precipitation was below the annual precipitation average and at the start of 2013, precipitation was above the average mean (ISGS, 2013). The January-August 2012 statewide temperature was 10.5°C (50.9°F), 4.2 degrees above normal (ISGS, 2012). The beginning of 2013 started off with a temperature of -0.11 °C (31.8°F), 2.8° above average.

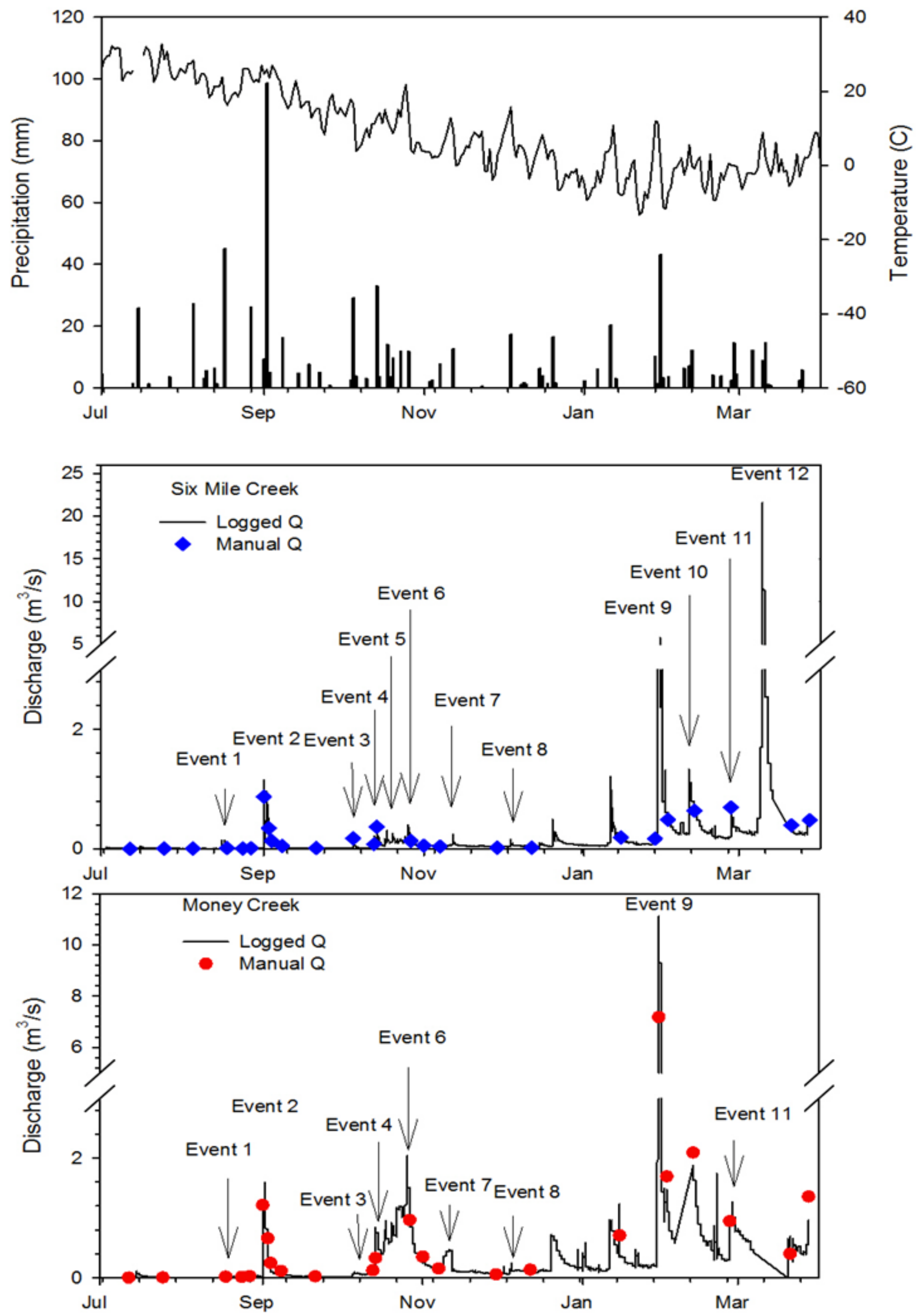

Figure 5: (a) Precipitation and temperature (precipitation and temperature data from NOAA.com, http://www.ncdc.noaa.gov/cdo-web/faq_cdo#GHCND, Station: Normal 4 NE IL US), and hydrograph, manual baseflow and storm flow discharge measurements and continuously logged discharge on (b) SMC and (c) MC from July 12, 2012 to March 28, 2013. No data was collected on SMC during Mar.14-21 or on MC from Aug.6-16, Oct.17-18 (Event 4), Feb.5-12 (Event 10), and between Mar.7-20 (Event 12) due to instrumentation error.

Generating the Rating Curves

Manual field baseflow and storm flow discharge measurements were plotted against manual stage measurements and used to convert continuous logged stage to discharge measurements using a rating curve. There were 10 baseflow and 16 storm Q measurements used to create the SMC rating curve. There were nine baseflow and 14 storm flow Q measurements used to create the MC rating curve. The established rating curves were used to generate discharge values from a continuously logged stage using a power relationship (Figure 6a and 6b). SMC data generated an equation of $y=2.3214x^{3.5369}$, with an R^2 value of 0.9672. The line generated by the data for MC was $y=3.551x^{2.6729}$, with an R^2 value of 0.9537.

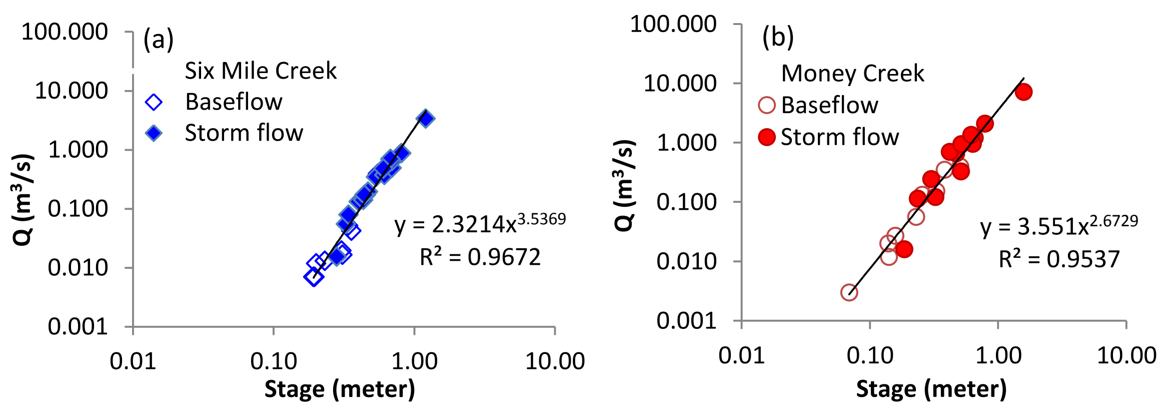

Figure 6: Rating curves for (a) SMC and (b) MC illustrating the relationship between stage (meter) and discharge (m^3/s).

Relationship between Turbidity and Suspended Sediment

For all manual baseflow and storm flow discharge measurements, turbidity and suspended sediment concentrations were taken. Turbidity and suspended sediment concentrations were represented by a power relationship on SMC and MC. The equation of the line generated by SMC was $y=2.7281x^{0.531}$, with an R^2 value of 0.8175 (Figure 7a). The equation of MC was $y=7.9332x^{0.2739}$, with an R^2 value of 0.2802 (Figure 7b).

Figures 7a and 7b show the suspended sediment concentrations in relationship to turbidity for the summer, autumn, and winter months. On SMC, the highest suspended sediment concentration corresponded to the higher turbidity seen in the winter. Turbidity would be an appropriate proxy for measuring suspended sediment on SMC. On MC, the highest suspended sediment concentrations did not correspond to the highest turbidity, indicating that there was less of a relationship between suspended sediment and turbidity on MC than SMC.

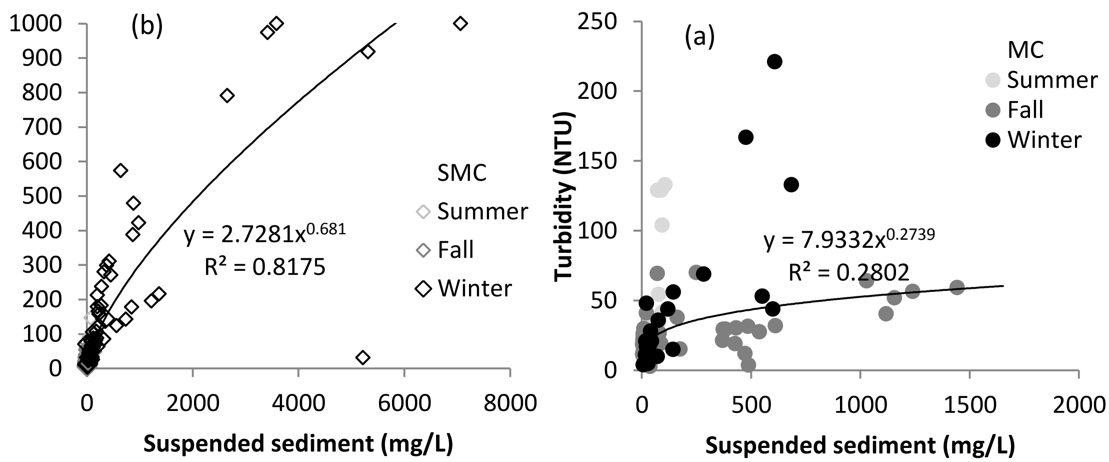

Figure 7: Suspended sediment concentrations versus turbidity on (a) SMC and (b) MC during baseflow and storm flow.

Baseflow

Baseflow conditions were monitored Jul.25, Aug.5, Aug.24, Aug.28, Sept.21, Nov.1, Nov.7, Nov.29, Dec.12 and Mar.21 on SMC and MC. During baseflow, the means of all measured parameters, except for stage, were higher on MC than SMC (Table 2). The cross sectional area of SMC was about a third of the cross sectional area of MC, thus the average stage was higher on SMC because it encompasses a smaller area, but provides similar discharge during baseflow. No statistical differences were found between baseflow TSS, Q, TSS load, or TSS load/drainage area on each stream (Appendix B).

Discharge

During baseflow, Q ranged from 0.00-0.39 m^3/s on SMC and from 0.00-0.40 m^3/s on MC. Overall, the average baseflow Q was two times higher on MC than SMC (Table 2).

Suspended Sediment

TSS was also twice as high on MC, 25.55 mg/L, compared to 11.7 mg/L on SMC (Table 2). Turbidity was almost twice as on high MC, 25.55 NTU compared to 14.65 NTU on SMC (Table 2). Both streams had similar average inorganic and organic percentage compositions of TSS. On SMC the average baseflow percentage of inorganic suspended sediment was 75.44% and the organic suspended sediment percentage was 24.56%. On MC, the average inorganic percentage was 77.41% and the average organic percentage was 22.59% (Appendix C).

Suspended Sediment Load

Although Q, turbidity, and TSS load were higher on MC, SMC had a sediment load per drainage area (17 kg/m^2s) that was more than twice the load on MC during baseflow conditions (7.4 kg/ m^2s) (Table 2).

Nutrients

Average nitrate as nitrogen (NO_3-N) concentrations on MC (11.08 mg/L) was more than times the concentration on SMC (2.99 mg/L) (Table 2). Correspondingly, the nitrate load on MC was an order of magnitude higher compared to SMC. It was determined that baseflow did not contribution to the NO_3 loading occurring on SMC and MC (Appendices D and F).

The chloride concentration were slightly elevated on MC, 53.99 mg/L compared to 40.54 mg/L on SMC (Table 2). The chloride loads generated by SMC and MC during the study period were of the same magnitude, but MC had a larger chloride load.

Table 2: Mean baseflow conditions on SMC and MC (±standard deviation) (July 12, 2012-March 28, 2013).

Mean baseflow conditions (±standard deviation)			
	Six Mile Creek	Money Creek	units
Stage	0.29 (±0.54)	0.25 (±0.5)	m
	0.94 (±0.97)	0.81 (±0.9)	ft
Discharge	0.06 (±0.24)	0.13 (±0.36)	m^3/s
	2.01 (±1.42)	4.53 (±2.13)	ft^3/s
Turbidity	14.65 (±3.83)	26.76 (±5.17)	NTU
Total suspended sediment	11.7 (±3.42)	25.55 (±5.37)	mg/L
Organic sediment concentration	2.87 (±1.7)	5.77 (±2.4)	mg/L
Inorganic sediment concentration	8.83 (±2.97)	19.78(±4.45)	mg/L
Suspended sediment load	782 (±28)	861 (±29)	mg/s
Suspended sediment load/drainage area	17 (±4.1)	7.4 (±2.7)	kg/m^2s
$N0_3$-N concentration	2.99 (±1.73)	11.08(±3.33)	mg/L
$N0_3$-N load	$1.79x10^2$ (±13)	$1.44x10^3$ (±38)	kg
Cl^- concentration	40.54(±6.37)	53.99(±7.35)	mg/L
Cl^- load	$2.43x10^3$(±49)	$7.02x10^3$ (±85)	kg

Storm Events

Discharge, TSS concentrations and TSS load varied seasonally on SMC and MC. Discharge was generally twice as high on MC compared to SMC, with increasing Q and TSS loads in the late winter/early spring (Table 3 and 4). Seasonal variations indicate that TSS loads are two-four magnitudes higher in the late winter and early spring, which corresponds to Q being one to two magnitudes higher in both sub-watersheds. The highest TSS loads were seen during the highest peak Q events on both streams.

The first storm event (Event 1) began on Aug.17-18 and the last event (Event 12) was captured on Mar.10-12 (Figures 5b and 5c). No storm flow data were collected between Dec.15 – Jan.14 because of Illinois State University winter break. Equipment malfunction resulted in no data being collected on SMC (Figure 5b) during Mar.14-21 or on MC (Figure 5c) from Aug.6-16, Oct.17-18 (Event 5), Jan.29-31 (Event 9), Feb.5-12 (Event 10), and between Mar.7-20 (Event 12).

Discharge

Storm discharge ranged widely on SMC and MC during the study period. Q ranged from almost no flow at the beginning of the study period to near bank full flow in the spring on SMC, from 0.002-21.438 m^3/s and from 0.012-10.6 m^3/s on MC. The storm events that generated the largest Q on SMC, Jan.29-31 and Mar.10-12 were not captured on MC. Discharge was the highest in the early spring on both streams during the study period (Table 5b and 5c).

Suspended sediment

Suspended sediment concentrations ranged throughout the study period during the storm events. On both streams, the average TSS per storm was the lowest in the fall and increased over the duration of the study period, peaking in the late winter/early spring. TSS peaked on SMC between Jan.29-31 (2,127.2 mg/L) (Appendix D). The highest average TSS per storm on MC was in the fall between Oct.26-29 (583.5 mg/L) (Appendix E). The average sediment flux ranged two-four magnitudes on SMC from 16 to 1.80×10^5 mg/s and on MC from 19 to28.5×10^4 mg/s (Appendices D and E). Comparative data between the two streams was missing for multiple storm events.

Suspended Sediment Load

Suspended sediment loads ranged three to four orders of magnitudes on SMC from 2 to 2.93×10^4 kg and on MC from 2 to 2.05×10^3 kg (Table 3). Of the eight events collected on both SMC and MC, the load on MC ranged from 4-150 times larger than loads on SMC. There was a large sediment load increase in the late winter/early spring on both SMC and MC. On SMC, Jan.29-31 and Mar.10-12 storms contributed almost all the sediment load, but neither event was successfully captured on MC due to instrumentation malfunction, which has skewed the results moving forward. The final storm, Mar.10-12 was the largest spring precipitation event on SMC and generated a load 13 times larger than any previous event ($7.30x10^4$ kg) (Table 3). The highest TSS loads were seen in the spring on SMC and were projected to be similar on MC with further data collection (Table 3). From the data collected over the study period, SMC generated a larger total TSS load that was two magnitudes larger than MC (Table 3). Coinciding, SMC had a much higher TSS load per drainage area then MC (Appendices F and G).

Table 3: Total suspended sediment load per storm event and type of hysteresis pattern for SMC and MC (n.a. - data not available due to instrumentation malfunction).

Event	Period	SMC		MC	
		TSS load per storm (kg)	Hysteresis pattern	TSS load per storm (kg)	Hysteresis pattern
Event 1	Aug.16-17	7	random	3	clockwise
Event 2	Sept.1-4	213	double clockwise	898	clockwise
Event 3	Oct.5-6	2	clockwise	2	random
Event 4	Oct.13-17	19	random	213	random
Event 5	Oct.17-21	12	random	n.a.	n.a.
Event 6	Oct.26-29	13	random/clockwise	$2.05x10^3$	anti-clockwise
Event 7	Oct.9-12	7	counter-clockwise	34	anti-clockwise
Event 8	Dec.2-6	5	random	8	anti-clockwise
Event 9	Jan.29-31	$2.93x10^4$	clockwise	n.a.	n.a.
Event 10	Feb.10-12	442	anti-clockwise figure eight	n.a.	n.a.
Event 11	Feb.26-28	88	anti-clockwise figure eight	96	clockwise/no pattern
Event 12	Mar.10-12	$7.30x10^4$	clockwise	n.a.	n.a.
Total TSS/storm event (kg)		$1.03x10^5$		$3.75x10^3$	

Relationship between Discharge and Suspended Sediment load

In general, with increasing discharge, there was an increase in TSS load during the study period, with loads substantially increasing the spring on SMC and MC (Figure 5a-5c and Table 3). TSS loads and Q varied in the autumn on both streams, both TSS loads and Q were reduced in the winter, and then both increased considerably in the spring (Table 3). Overall, MC had higher Q values that corresponded to higher TSS loads compared to SMC during storm events (Table 4).

The highest peak Q generated the largest TSS load on SMC during the spring on Mar.10-12. The largest Q event on MC was on Jan.29-31, but the largest load on MC was seen in the fall on Oct.26-29 (because of limited data). The storm events on Oct, 17-21, Oct.26-29, Nov.9-12, and Dec.2-5 have no manual storm discharge measurements. Based on the data available, it was predicted that with further storm event analysis that MC would transport the largest loads in the spring during high Q.

When compared between the two streams, peak Q of each storm event varied widely between SMC and MC. The remnants of Hurricane Isaac during Sept.1-4 were the only events with a comparable peak Q values between the streams. Discharge was 1.15 m^3/s on SMC and 1.57 m^3/s on MC, but MC had a load that was more than four times greater than SMC (Table 3).

On SMC there were comparable peak Q storm events on Oct.26-29 of 0.40 of m^3s and 0.64 m^3/s during Feb.26-28, but the February event produced a load four times larger of 88kg compared to 13kg in the fall (Tables 3 and 4). Similarly, on Sept.1-4, SMC generated a peak Q of 1.15 m^3/s and on Feb.10-12, a peak Q of 1.33 m^3/s. Feb.10-12 had a TSS load that was 442 kg, twice as high as the fall load on Sept.1-4 of 213 kg.

There were similar peak storm Q on MC between Oct.5-6 of 0.11 m^3/s and on Dec.2-6 of 0.19 m^3/s, but the December event had a load of 8 kg, which was four times larger than 2 kg during the October event. On MC the peak Q during Sept.1-4 of 1.57 m^3/s was similar to Feb.26-28 of 1.255 m^3/s. In the fall, the Sept.1-4 event transported 898 kg, nine times more sediment than the comparable peak Q on Feb.26-28 of 96 kg. This was the only peak Q storm event comparison where a larger load was seen in the fall than winter/spring between the same stream.

The majority of suspended sediment transport occurred during storm events on both SMC and MC (Figure 8). SMC transported 99.76% (1.03×10^5 kg) of total TSS during storms and and MC transported 92.56% (3.57×10^3 kg) during storm events (Appendices F and G). On SMC, Jan.29-31 contributed 28.33% and Mar.10-12 contributed 70.65% of the total TSS load transported. On MC, Sept.1-4 contributed 25.18% and Oct.26-29 contributed 57.41% of total TSS load. The two largest TSS loads on SMC were not successfully collected on MC which as skewed the graphical representation in Figure 8. Overall, due to missing storm event data, these are conservative estimates indicating that the majority of TSS load was generated during storm events on both streams.

Table 4: Manual storm flow discharge measurements on SMC and MC and the storm event each discharge measurement corresponds to (August 2012-March 2013) (n.a. - data not available due to instrumentation malfunction).

		Six Mile Creek		Money Creek	
Event	Date	DISCHARGE (ft^3/s)	DISCHARGE (m^3/s)	DISCHARGE (ft^3/s)	DISCHARGE (m^3/s)
Event 1	August 18, 2012	0.54	0.02	0.57	0.02
	September 1, 2012	31.78	0.88	42.92	1.21
	September 3, 2012	12.24	0.35	23.28	0.66
	September 4, 2012	4.67	0.13	8.67	0.25
	September 8, 2012	1.93	0.05	4.06	0.11
Event 2	October 5, 2012	6.13	0.17	n.a.	n.a.
	October 13, 2012	2.80	0.08	4.33	0.12
Event 3	October 14, 2012	13.09	0.37	11.62	0.33
Event 4	October 27, 2012	4.94	0.14	34.09	0.96
No associated event	January 15, 2013	6.84	0.19	25.02	0.71
	January 28, 2013	6.07	0.17	n.a.	n.a.
	January 30, 2013	118.96	3.37	253.68	7.18
Event 9	February 2, 2013	17.41	0.49	59.89	1.69
Event 10	February 12, 2013	22.56	0.64	74.02	2.09
Event 11	February 26, 2013	24.50	0.69	33.35	0.94
Event 12	March 28, 2013	16.87	0.48	47.87	1.35

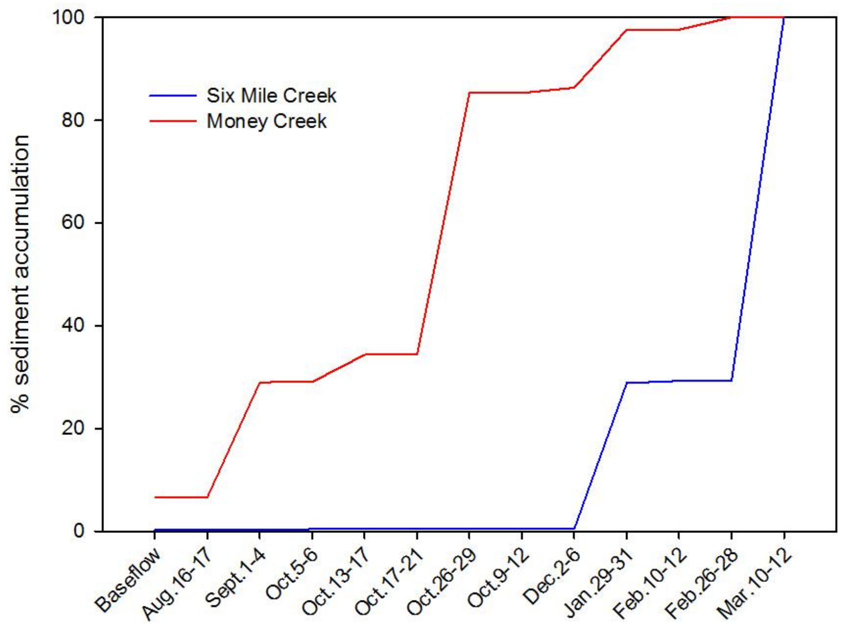

Figure 8: Percentage of total suspended sediment load accumulation from each storm event and baseflow on SMC and MC. The percent suspended sediment accumulation on MC was skewed due to multiple storm events not be successfully sampled.

Hysteresis

Multiple examples of TSS-Q hysteresis patterns were observed in both sub-watersheds. Of the 12 storm events on SMC, the number and type of hysteresis was as follows: four had clockwise hysteresis patterns, two displayed an anti-clockwise figure-eight pattern, one displayed counter-clockwise hysteresis, one displayed a double clockwise pattern, and four had no discernible pattern (Table 3). Of the nine storm event samples on MC: three were an anti-clockwise, two were clockwise, three had no pattern and one did not have enough samples collected to discern a pattern (Table 3).

Figure 9 displays examples of common hysteresis patterns seen in the stream systems with hydrographs and TSS concentrations. The clockwise pattern (Figure 9a) on SMC indicates a peak in TSS before peak Q, as TSS increased on the rising limb and decreased on the falling limb. Sediment was flushed through the system on the rising limb and the sediment supply was exhausted on the falling limb, resulting in a decline in TSS. The double clockwise loop (Figure 9b) on SMC resulted from two sediment peaks leading the two hydrograph peaks. TSS was not as high on the second rising limb, though the increase in sediment again indicated a reliable source of sediment in the stream system. Both Figures 9a and 9b indicate that the majority of TSS came with the initial flush of flow through the system. An example of a random hysteresis pattern on MC (Figure 9c) shows multiple sediment peaks occur without any distinct relationship to the hydrograph peaks, resulting in no discernible hysteresis pattern. The anti-clockwise hysteresis (Figure 9d) displayed a peak sediment lag behind peak Q on MC.

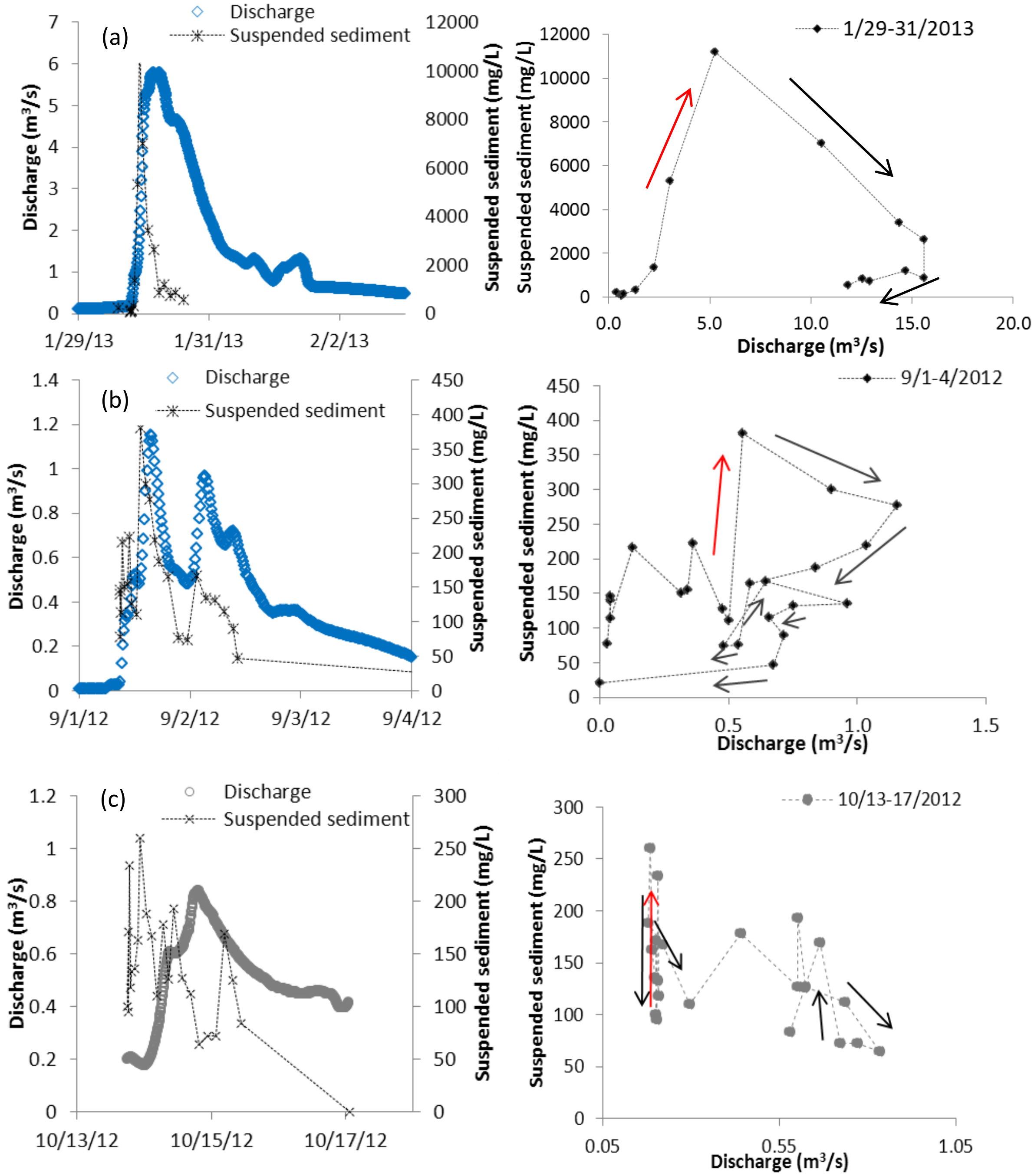

Figure 9: Starting from the top right, event hydrograph, TSS, and hysteresis loops for (a) clockwise hysteresis pattern on SMC (b) double loop clockwise hysteresis pattern on SMC (c) a random hysteresis pattern on MC, and (d) a counter-clockwise hysteresis loop on MC. *Note-the red arrow indicates the initial direction of the hysteresis pattern on the Q vs. TSS graphs. Figure 4d is continued on the next page.

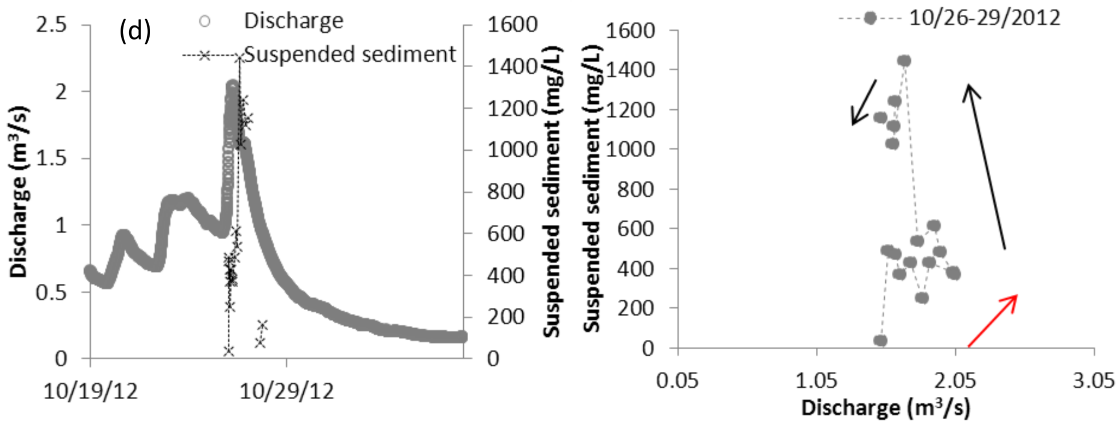

Six Mile Creek Hysteresis

At the beginning of the study period on SMC, high precipitation events generated clockwise hysteresis patterns. Hysteresis patterns in the late autumn and early winter were random/anti-clockwise and clockwise patterns were seen in the spring. The storm event on Sept.1-4 was generated by the remnants of Hurricane Isaac. The subsequent events on Oct.13-15, Oct.17-21, Oct.26-29, and Nov.12-14 consisted of random hysteresis patterns with TSS loads a tenth-twentieth of the load transported by Hurricane Isaac storms (Appendix D). The hydrograph of Sept.1-4 indicates that there were two peaks in discharge and subsequently, two peaks in suspended sediment concentration, which generated the double clockwise pattern (Figure 9b). In the spring, the Jan.29-31 event generated a clockwise hysteresis pattern and transported a TSS load substantially higher than the following sediment loads on Feb.10-12 and Feb.26-28 (Table 3, Appendix D). Feb.10-12 and Feb.26-28 events generated anti-clockwise hysteresis patterns. The final storm, Mar.10-12 was the largest spring precipitation event on SMC and generated a clockwise hysteresis pattern.

Overall, on SMC, the medium to larger events (0.40-21.35 m^3/s) consisted of mainly clockwise hysteresis, with random patterns for smaller events (0.148-0.45 m^3/s), which was consistent with Smith and Dragovich (2008) (Table 3, Appendix D). The counter clockwise patterns were evident between the small-medium events (0.64-1.33m^3/s) on SMC.

Money Creek Hysteresis

At the beginning of the study period on MC, similar to SMC, high precipitation events generated clockwise hysteresis patterns. The rest of the study period was a mix of random and anti-clockwise patterns, with the random patterns following large precipitation events. Sept.1-4 was the largest precipitation event in the fall which was the remnants of Hurricane Isaac. The hydrograph of Sept.1-4 displayed a clockwise hysteresis pattern with two peaks in discharge, and subsequently two peaks in suspended sediment concentration, though the initial Q peak had a TSS concentration that was eight times larger than with the second increase in Q (Appendix E). The TSS concentrations of Oct.5-6 and Oct.13-17 peaked at concentrations two-six times lower than Sept.1-4 and the TSS loads were a tenth of Sept.1-4 (Table 3). The storm event on Oct.26-29 transported a load of sediment 13 times larger than the following storms on Nov.9-12 and Dec.2-5. All three events, Oct.26-29, Nov.9-12, and Dec.2-5 had anti-clockwise hysteresis patterns.

On MC, the medium to larger events (0.47-10.6m^3/s) generated anti-clockwise patterns, with random hysteresis patterns for smaller events (0.10-0.84 m^3/s). The clockwise patterns occurred at a range of Q from 0.04-1.26 m^3/s.

Sediment Accumulation in the Lake Bloomington Reservoir

A conservative overestimate of the length of time required for the total TSS load on SMC and MC during this study period was used to determine how long it would take for the sediment to fill in the reservoirs (Table 5). The sub-watershed of MC contributed 44.9 m^3 per year of sediment which would fill in Evergreen Lake in $4.25x10^5$ years. The sub-watershed of MC generated 1.7 m^3 of sediment per year requiring 5.21x10^6 years to fill in Lake Bloomington, but as the storm data are incomplete, this was not representative of the actual volume. This estimate was an overestimate of how long it would take Lake Bloomington to fill in from sediment upstream.

The original storage capacity of Lake Bloomington was 9.10x10^6 m^3 (7,380 acre-feet) in 1929, and when the lake had a bathymetric map contracted in 1999, it was determined that the storage capacity was 8.35x10^6 m^3 (6,768 acre-feet). Over the 70 year span, there was a sediment accumulation rate of 1.08x10^4 m^3/year (8.75 acre-feet) (Table 5). This was compared to the sediment infilling rate determined during the current study period (1.7 m^3) on MC (Table 5). A conservative sediment accumulation rate, 122 m^3/year was determined for the past 70 years that the sub-watershed of MC contributed to Lake Bloomington (Table 6). No bathymetric mapping has been conducted on SMC so no volume estimates were made. There has also been no dredging in Lake Bloomington to remove the accumulated sediment.

Table 5: Original storage capacity and TSS loads for baseflow and storm flow used to determine the rate of reservoir sediment infilling from SMC and MC sub-watersheds, McLean County, IL, US.

Reservoir infilling	Evergreen Lake	Lake Bloomingt	Units
Original storage capacity	1.91x10^7	9.10x10^6	m^3
Total TSS load	1.03x10^5	4.02x10^3	kg/yr
Silicate particle density	2.3	2.3	g/cm^3
Sediment filling in	45	1.7	m^3/yr
# of years for reservoir to fill in	4.25x10^5	5.21x10^6	years

Table 6: Comparison of the change in original storage capacity (1929) to the bathymetric storage capacity (1999) on MC looking at the sediment accumulation rate of this study compared to the sediment accumulative rate from the previous work.

Historical sediment input to reservoir	Lake Bloomington	Units
Original storage capacity (1929)	9.10×10^{6}	m^3
Bathymetric mapping storage capacity (1999)	8.35×10^{6}	m^3
Amount of storage capacity lost between 1929-1999 (70 years)	7.55×10^{5}	m^3
Amount of sediment accumulated/year between 1929-1999	1.08×10^{4}	m^3
Total sediment accumulation/70 years from current study	1222	m^3

Nutrients

Nitrate and chloride concentrations and loads were measured on storm samples from the 12 storms on SMC and eight storm events on MC (Table 7, Figures 10a and 10b). On MC, Events Oct. 17-21, Jan.29-23, Feb.26-28, and Mar.10-12 were not collected and therefore did not have nutrient compositions analyzed. In Figure 7, on MC during Aug.16-18, b.d. indicates that all nitrate concentrations were below the detection limit of the Ion chromatograph (0.79 mg/L). In Figure 7, the grey shaded boxes indicate chloride concentrations that were below the detection limit of 13.38 mg/L.

The average NO_3-N storm concentration varied on SMC from 0.89 mg/L during Sept.1-4 to 12.1 mg/L on Mar.10-12 (Table 7). On MC, the average NO_3-N storm concentration ranged from 0.34 mg/L on Oct.5-6 to 8.22 mg/L on Feb.26-28. The Feb. 10-12, Feb.26-28, and Mar.10-12 storm events on SMC were the only events that the NO_3-N concentrations exceeded the acceptable EPA NO_3-N drinking water standard of 10 mg/L seen during this study period (Table 7); concentrations for MC never exceeded the standard. Nitrate concentrations were seen to peak in the late winter/early spring on both streams (Table 7 and Figure 10a).

Nitrate loading occurred entirely during storm events on both streams (Figure 11a). MC transported a nitrate load of 1.84×10^4 kg, slightly larger than the load on SMC of 1.36×10^4 kg (Appendices D and F). However, when the drainage area was considered, SMC transported 289 kg/km², almost twice the NO_3-N load on MC of 163 kg/km². Nitrate loading increased one order magnitude during the spring time on SMC to a magnitude of three, which was the highest load seen during the study period (Appendix D). Nitrate loading on MC appeared to remain consistent throughout the study period during storm events at a magnitude ranging from two to three (Appendix F).

The average chloride storm concentration varied on SMC from 25.71 mg/L on Sept. 1-4 to 220.59 mg/L on Jan.29-31. On MC, the storm chloride concentration ranged from 16.33 mg/L on Nov.9-11 to 103.2 mg/L on Jan.29-31. At no point during this study period were chloride concentrations seen above the EPA drinking water standard of 250 mg/L on either stream. Chloride concentrations peaked in the winter on both streams (Table 7, Figure 10b).

Storm events accounted for all chloride loading on both streams (Figure 11b). Storm events on SMC transported a chloride load of 1.42×10^5 kg, compared to the storm chloride load of 2.36×10^4 kg on MC (Appendices E and G). However, when drainage area was accounted for, MC transported only 217 kg/km² of chloride, while SMC transported 3,012 kg/km². On SMC, the chloride load on Jan.29-31 was two magnitudes larger than any other storm event chloride load. On MC, the chloride loads ranged one to three orders of magnitude in the fall, but were consistent an order of magnitude of three in the winter (Appendix G). Interestingly, the largest chloride load on MC was as a magnitude of four, one order larger than any other event which occurred in the fall (Sept. 1-4).

Table 7: Average nitrate as nitrogen and chloride concentrations during the storm events on SMC and MC. *Note-grey cells are chloride concentrations that were found to be below the range on the standard curve (b.d. – data was below the detection limit and n.a. - data not available due to instrumentation malfunction).

		Six Mile Creek		Money Creek	
		NO_3	Cl^-	NO_3	Cl^-
STORM EVENT	Period	mg/L	mg/L	mg/L	mg/L
Event 1	Aug.16-17	1.04	36.57	b.d.	27.89
Event 2	Sept.1-4	0.89	25.71	1.16	54.45
Event 3	Oct.5-6	1.05	33.78	0.34	34.33
Event 4	Oct.13-17	1.11	63.85	0.86	103.20
Event 5	Oct.17-21	1.72	67.85	n.a.	n.a.
Event 6	Oct.26-29	1.60	38.57	4.79	34.97
Event 7	Nov.9-12	1.75	80.10	4.95	16.33
Event 8	Dec.2-6	1.60	58.85	5.87	33.22
Event 9	Jan.29-31	7.97	220.59	n.a.	n.a.
Event 10	Feb.10-12	10.34	17.6	n.a.	n.a.
Event 11	Feb.26-28	10.63	73.1	8.22	22.33
Event 12	Mar.10-12	12.10	52.0	n.a.	n.a.

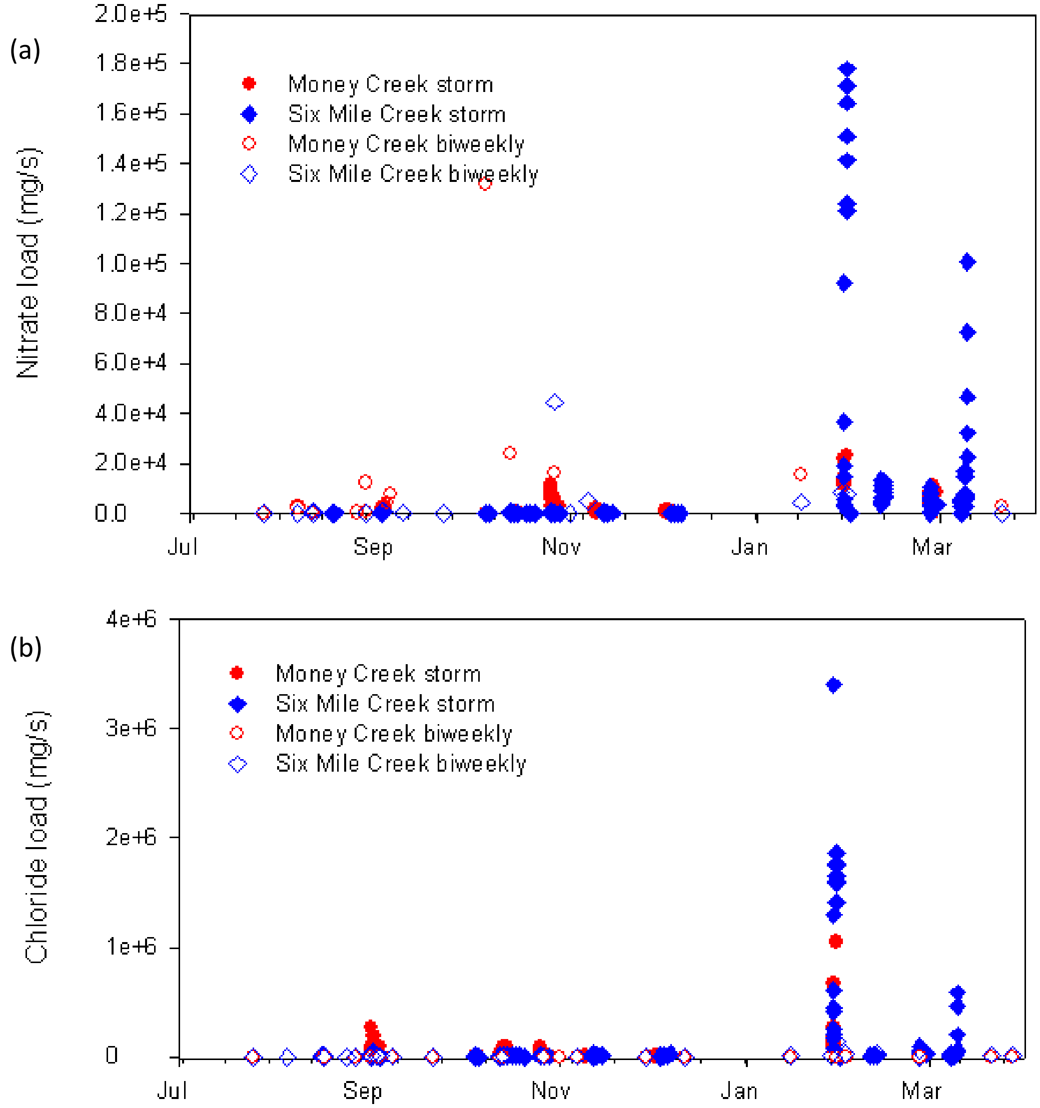

Figure 10: Nitrate and chloride loads (mg/s) for baseflow and storm flow events on (a) SMC and (b) MC.

(a)

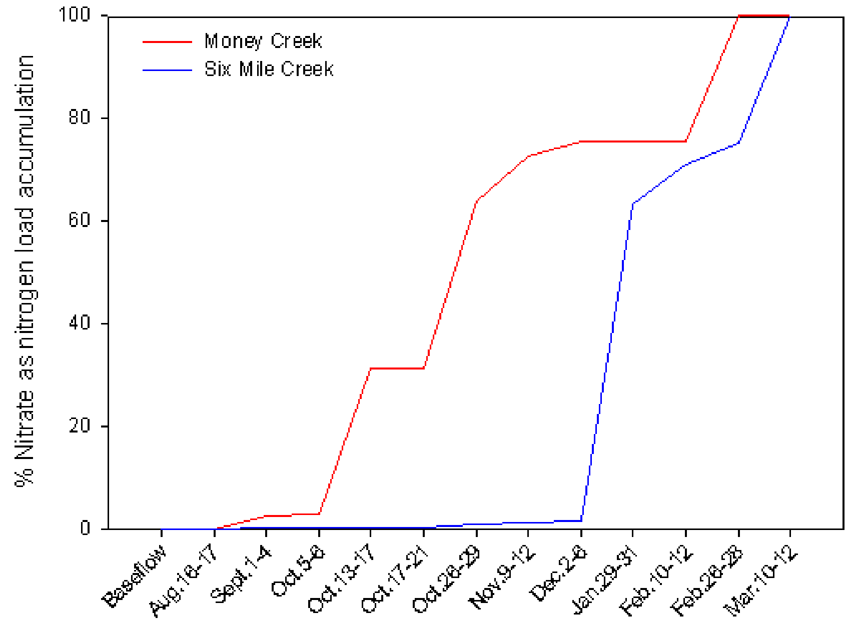

(b)

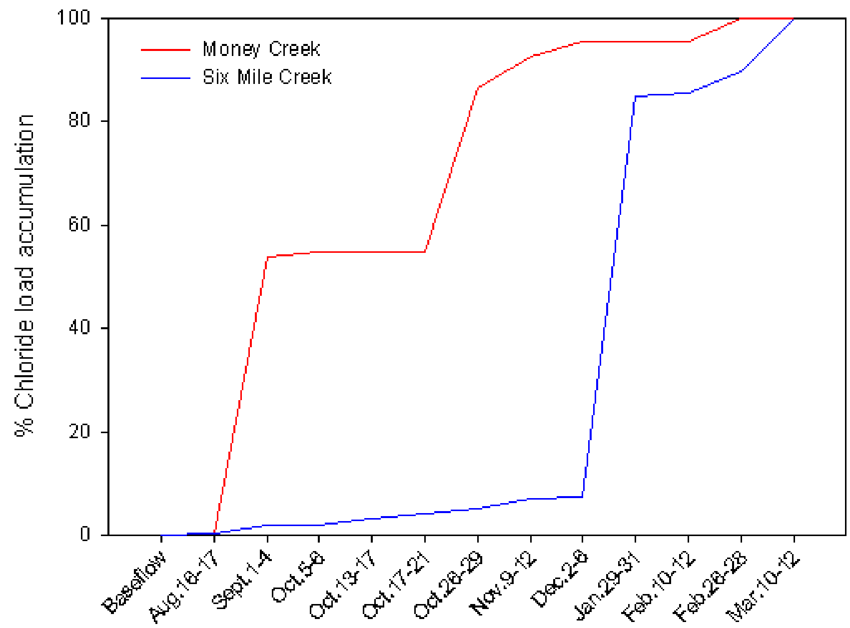

Figure 11: Percentage of total nitrate as nitrogen and chloride load accumulation from each storm event and baseflow on (a) SMC and (b) MC. The percent of nutrient accumulation on MC was skewed due to multiple storm events not be successfully sampled.

CHAPTER IV

DISCUSSION

Seasonal Changes

The study period was unique as at the start of the study McLean County, IL was in drought conditions. During the drought conditions in fall 2012, rain events were of larger magnitude, but discharge was lower, suggesting less overland run-off (Figures 5a-c). When precipitation occurred, rainfall was absorbed by agriculture and other vegetation, infiltrated into groundwater, or underwent evapotranspiration, contributing to low stream discharges seen in late summer/early autumn. This was evident for both streams as the lowest storm event Q occurred in the autumn also corresponded to the smallest sediment loads (Table 3).

Between September, 2012 and March, 2013, precipitation events occurred regularly, reducing the drought conditions to average precipitation conditions by the end of the study period. In the autumn, after the crops were harvested, conditions were more favorable to soil erosion and sediment transport, which is similar to the findings of Lecce et al. (2006). There were frequent storm events directly before and following Oct.26-29 on MC, the Oct.26-29 storm had the largest peak Q in the fall which transported the largest load seen during the study period (Figures 5a and 5c and Tables 3 and 4). The high Q in the fall on MC transported the available sediment within the stream channel and the TSS load was likely increased by external soil erosion from croplands. This was not seen to occur on SMC during the fall as there minimal discharge during Oct.26-29 on SMC (Table 5b).

As the seasons changed, smaller precipitation events generated larger peak discharges in the late winter and early spring. During winter and early spring the ground was frozen, likely inhibiting infiltration and increasing the chance of sheetflow and overland flow due to snowmelt and spring rain (Gao and Josefson, 2012). Overland flow likely contributed to the elevated TSS loads seen on SMC in the later winter/early spring as there were no crops on the ground and the temperature fluctuated above and below 0^{o}C between late December and early March, allowing for potential soil erosion (Table5a). The data collected from SMC and MC indicate that during the winter/early spring, smaller precipitation events generated higher Q events and higher TSS loads (Table 5a-c, Appendix J and K).

Baseflow

At baseflow, discharge was similar between the two streams. There were no statistically significant differences between the two streams, which was not expected as the sub-watersheds have different gradients and drainage areas (Table 1). MC transported twice the TSS load compared to SMC, but SMC had a larger standard deviation, indicating that the supply of sediment varied more widely during baseflow conditions on SMC than with MC. However, when the drainage area was accounted for, SMC had a TSS load that was twice as high as MC (Table 2). Proportionally, SMC was generating more baseflow suspended sediment per drainage area than MC. Based on the data collected, I accept the hypothesis that SMC generated twice as much TSS than MC during baseflow.

The percent organic and inorganic suspended sediment appeared consistent throughout the study period. The percentages of organic and inorganic sediment were comparable between the streams, which indicate that the source of sediment was similar. Both sub-watersheds have a high percentage of agricultural land use that was likely the contributing source as the compositions were almost identical.

When the historical TSS and TSS data collected during the study period were compared, the range of suspended sediment concentrations recorded during this study period was in line with the historical data on SMC and MC (Figure 11a and 11b). This indicates that the supply of TSS has remained a steady input into both streams.

There was no significant difference when comparing the historical data between (January 2005- April 2012) to the suspended sediment data collected during the study period (July 2012-March 2013) using a two-tailed t-test, $t(238)=-1.03$, $p<0.303$. (*Note-there is no separation of biweekly and storm events for the historical data).

Similar to Royer et al. (2006), elevated nutrient concentrations were seen in the late winter and spring (Figure 10). Storm flow accounted for 100% of nitrate and chloride loading on both streams, which was likely enhanced by the highly tile drained watersheds (Appendices D-G). This is similar to literature as Drewry et al. (2009) in Australia and Royer et al. (2006) in Illinois found that nutrient loading occurred above median discharge. The tile drains significantly increase the rate at which the water runs over the ground surface and into the streams, contributing any soluble nutrients that are available from the top soil.

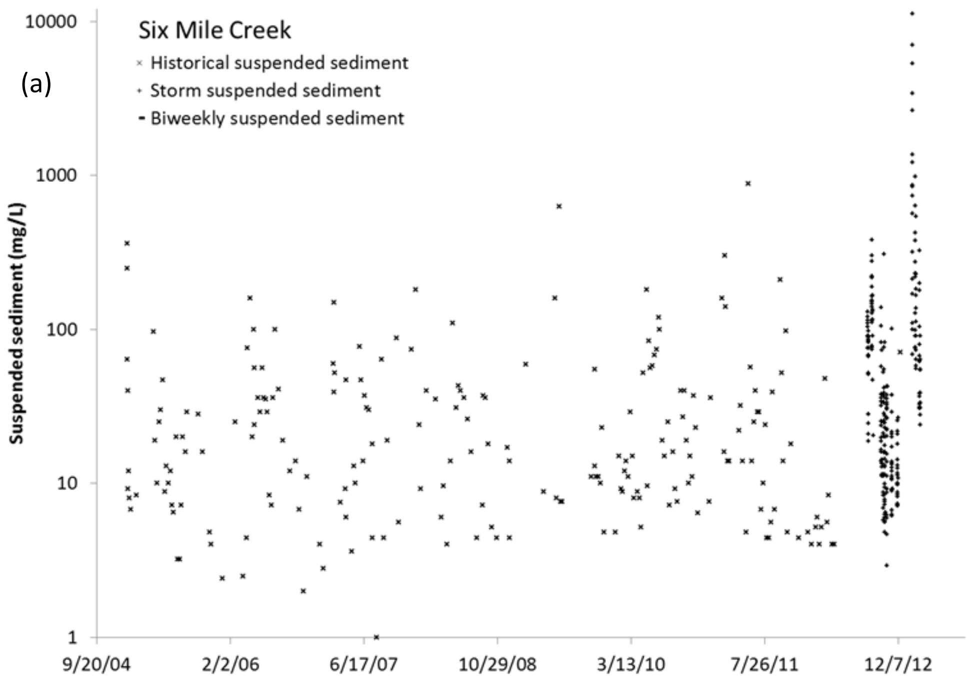

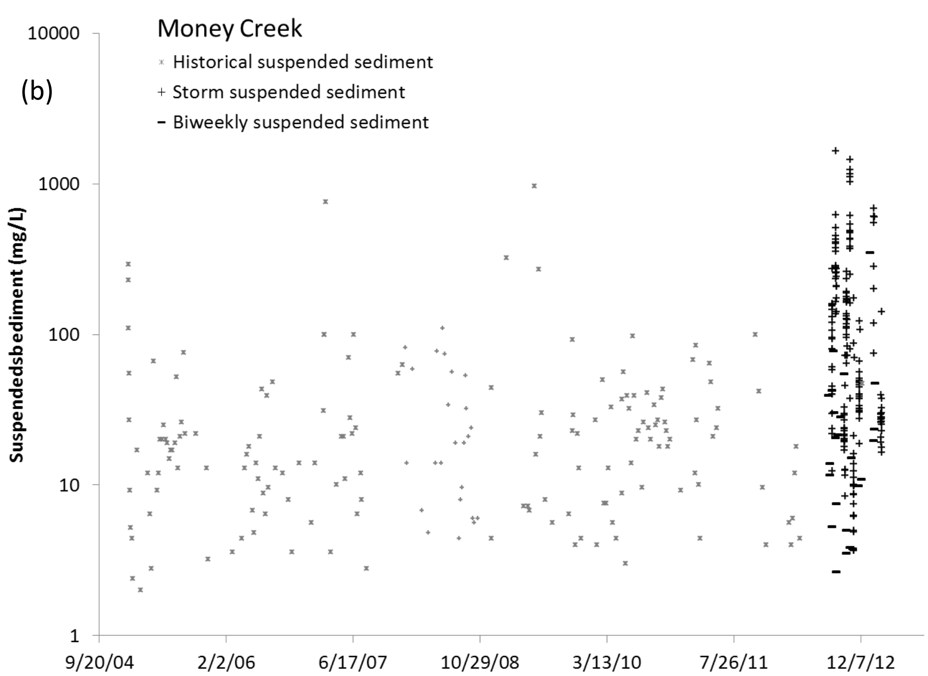

Figure 12: Historical suspended sediment data (September 2004- July 2012) and suspended sediment data collected during the study period (July 2012-March 2013) on (a) SMC and (b) MC.

Storm Flow

Relationship between Q, Turbidity, and SS

Statistical relationships linking TSS and turbidity, which are influenced by Q, are commonly reported in literature (Drewry et al., 2009, Loperfido et al., 2010). On MC, there was higher Q throughout the study period and also a higher average TSS and turbidity compared to SMC (Table 2). Turbidity increases with increasing Q, so it was expected that with a higher Q, there would be more turbidity. SMC had a strong correlation between TSS and turbidity, indicating that turbidity is an appropriate indicator of suspended sediment concentrations (Figure 7a). MC had a much weaker correlation between turbidity and TSS, potentially because of the changing weather conditions seen in the fall and winter (Figures 5c and 7b). Loperfido et al. (2010) found that TSS was well correlated to turbidity in southeastern Iowa. Drewry et al. (2009) also found that turbidity was highly correlated to TSS concentrations in southeast Australia using a linear relationship, which was different than the power relationship seen on both SMC and MC.

Total Suspended Sediment Load

SMC had a more complete TSS load record for the duration of the study period, while MC's was incomplete due to instrumentation malfunction. Based on the data presented, all of the TSS load was generated during storm events on SMC and almost all of the TSS load was generated from storms on MC, which is similar to other streams (Gao and Josefson, 2012, Drewry et al.,2010, and Fraley et al.,2009).

The sediment load on SMC was visibly higher in the late winter/early spring, and I infer, considering that the TSS loads on MC were constantly two-four magnitudes larger than SMC during multiple storm events, that with further data collection, MC would likely have a higher total TSS load than SMC (Tables 3 and 4).

Relationship between Discharge and TSS load

Overall, TSS loads increased with increasing Q on both streams. MC typically had a discharge that was twice that seen on SMC, which corresponded to higher TSS loads on MC during storm events. The higher Q and larger TSS loads was likely because of the larger sub-watershed area and larger percentage of agricultural land use potentially contributing to increased soil erosion on MC.

Hysteresis

Variations in the Q-TSS relationship during the study period are due to temporal variations in sediment availability and stream transport capacity. For the same Q, which controls stream transport capacity, TSS varies with availability of sediment (Lefrancois et al., 2007). When Q increases, the stream transport capacity increases, but if the sediment availability is limited, TSS may not increase. On the two streams studied, TSS loads increased with increasing Q, but there was also a decrease in sediment availability noticed in multiple storm events proceeding larger events (Appendices H and I).

Initially, SMC and MC displayed similar patterns of hysteresis in the fall of 2012 that consisted of clockwise hysteresis patterns. The clockwise patterns seen on both streams indicate a pre-existing source of sediment within the stream (Lenzi and Lorenzo, 2000). Field observations on SMC indicated that just upstream the sample site where the river bends is a cutbank, contributing a reliable sediment supply. The large precipitation event, in this case the Sept.1-4 storm event was generated by the remnants of Hurricane Isaac flushed both stream beds of sediment that had built up in the streambeds during the drought of the previous months

(Figure 5a-c and Table 3). Hurricane Isaac likely removed available sediment from both systems as subsequent events consisted of TSS concentrations that were half the concentration and loads that were only a tenth of the loads experienced during Hurricane Isaac on both streams (Table 3, Appendices H and I). Crops were still on the ground in early autumn, and even with sheetflow, there was likely minimal soil erosion occurring contributing to sediment transport so the sediment load seen was likely entirely from within the stream channel. There was the potential, that as it had been dry for so long, heavy rain falling over a short period of time would create overland flow and not infiltrate into the ground, potentially helping to explain for the large sediment load generated in the fall on MC during the Oct.26-28 storm event (Table 3, Appendix I).

Precipitation events occurred on average every two weeks through September and October which generated random hysteresis patterns during Oct.13-15, Oct.17-19, Oct. 26-29, and Nov. 12-14 on SMC and during Oct.5-7 and Oct.13-15 on MC. The random patterns and low TSS loads signifies that the small, but frequent storm events were transporting the available sediment from within the stream and because of the continuous precipitation, minimal sediment was able to be stored within the stream channel between storm events, resulting in the random hysteresis patterns on both streams. This persisted through the winter, allowing sediment to become stored in the stream channel.

After Hurricane Isaac, SMC and MC diverged slightly in hysteresis patterns. However, in the spring other large storm events came through and exhausted the sediment supply in following events on SMC and MC, as indicated by TSS concentrations and loads that were often less than half that of the prior event. On SMC, Jan.29-31 generated a clockwise pattern that probably flushed Feb.10-12 and Feb.26-28 of sediment (Table 3, Appendix H). Both Feb.10-12 and Feb.26-28 events demonstrated anti-clockwise hysteresis patterns, which are indicative of an increase/arrival of distant particles from upstream (Lefrancois et al., 2007) or from a new sediment source from channel incision. Kinney (2005) conducted an in-field streambank survey on SMC and found that channel incision was the primary factor influencing streambank erosion, generating 90% of the sediment entering Lake Evergreen.

On MC, the Oct.17-21 event transported the available sediment in the stream channel as the following storm events on Oct.26-29 and Nov.9-12 had much lower TSS loads (Table 3, Appendix I). All three events displayed anti-clockwise hysteresis patterns, which indicated a new sediment source had likely become available during the increased Q. Kinney (2006) conducted an in-field streambank survey on MC that found that the primary source of streambank erosion was from later bank migration. As Q increases, the erosion potential along the streambank increases, which could have contributed as a source of new sediment to the stream mid-storm event. Field observations indicated that there was lateral migration of the stream bed and with increases in Q, more lateral migration occurred ranging from 2.5-7.5cm. The Q flushing mechanism was a repeat pattern indicating the most sediment was transported in the initial onset of flow and the following storm events could only transport what sediment had become available in-between storm events. It is important to note that with the lateral migration, the stream bed profile may have changed which may influence the rating curve generated during this study on MC.

On SMC, the medium to larger events consisted of mainly clockwise hysteresis seen in the fall and spring, random patterns at smaller discharges during the winter. This pattern was similar to Smith and Dragovich (2009). The counter clockwise patterns were evident between a mix of small-medium events on SMC. These patterns are seen on SMC because with higher flow, more sediment was able to be transported from internal and external sources (Gao and Josefson, 2009). SMC is an actively incising stream, which created a reliable source of sediment for the stream as 61% of the banks were degrading or degrading and widening upstream throughout the sub-watershed (Kinney, 2005). The anti-clockwise patterns are indicative of a new sediment source developing during a storm event, which can happen at a range of discharges and at varying locations upstream, but determining those specific locations was outside the scope of this project.

On MC, the medium to larger events generated anti-clockwise patterns during the autumn and spring, with random hysteresis patterns for smaller discharges during the winter, and the clockwise patterns occurred at a range of Q throughout the study period. MC has a stable stream bed with a sub-watershed twice the size of SMC so it required more energy to transport sediment and to generate new sediment sources. The anti-clockwise pattern represent a release of sediment from somewhere within the stream channel, most likely from the lateral migration observed in the field near the sample site or upstream bank collapse. The random hysteresis indicated that the available sediment had been previously removed and no sediment coming in externally from overland or sheetflow.

Sediment Accumulation in the Lake Bloomington Reservoir

Using the original storage capacity and the previous bathymetric mapping of MC, an estimate of total sediment contribution from all tributaries upstream of the Lake Bloomington was calculated to be 1.08×10^4 m^3 per year of sediment accumulating. This was substantially higher than the total sediment load that the sub-watershed of MC was contributing per year, 1.7 m^3, determined by the duration of the study period. The amount of the sub-watersheds of SMC and MC are contributing is a very conservative underestimate of total sediment accumulation as the study period was not a full year and not all storm events were measured on either stream. At the current sediment accumulation rate, Lake Bloomington will take more than five million years to fill in. SMC was contributing 45m^3 of sediment to Evergreen Lake, which at that rate, would take Evergreen Lake just over 400,000 years to fill in. Both of these are well below the typical annual reservoir loss of 0.81-1.2% for Illinois reservoirs (Ackerman et al., 2009), but both are an overestimate of the reservoir lifetime.

Nutrients

Nutrient loading occurred entirely during storm flow, which is similar to other literature (Drewry et al., 2009 and Royer et al., 2006). During storm events there were only three events on SMC and none on MC that exceeded the EPA drinking water standards for NO_3-N levels and the EPA chloride standard was never exceeded on either stream.

The results indicated that when the drainage area was considered, SMC was transporting a chloride load 16 times larger than MC, which is likely due to the higher portion of developed land. This is also skewed from limited data sets on MC, but the hypothesis that MC will transport more chloride is rejected. The nitrate load was higher on SMC when the drainage area was considered refutes the hypothesis that MC would transport more nitrate as well. This is potentially because of the slightly higher percentage of agricultural land use in the SMC sub-watershed or because as SMC had been previously seen to transport more sediment, the increased sediment also could have led to increased nutrient loading (Kinney, 2006).

There were seasonal variations to both nitrate and chloride during this study period. The seasonal increase of nitrate loading on SMC during the spring was likely from nitrate leaching from the fertilizer applied in the agricultural fields, which is similar to other literature (Royer et al., 2006). Chloride concentrations and loads were seen to peak in the winter on SMC, but there was a consistent chloride load on MC, which may have been from chloride leaching out from the nearby soil, which will be looked at in future research, along with continued baseflow and storm flow monitoring.

CHAPTER V

CONCLUSION

It was postulated that because of different watershed characteristics, that the SMC and MC sub-watersheds would respond differently to precipitation events through discharge and TSS loads, which was seen throughout the study period. When the suspended sediment concentrations were compared during baseflow, it had been hypothesized that SMC would have a higher suspended sediment concentration than MC, which was found to be incorrect. However, when the drainage area was considered, SMC had a higher suspended sediment load per drainage area than MC during baseflow, so the hypothesis is accepted that SMC transported more TSS than MC.

It was hypothesized that suspended sediment concentrations would increase with increasing discharge during storm events, which was seen on both watersheds, though TSS loads were often dependent on sediment availability. MC was predicted to have higher Q because of the larger watershed, which was evident throughout the study as the Q on MC was usually twice the volume of SMC.

The hypotheses that MC would have higher nitrate as nitrogen and chloride concentrations than SMC were refuted. Both nitrate and chloride loads were larger on MC, but when the drainage area was considered, SMC transported twice as much nitrate and almost two times more chloride than MC. The sub-watershed on SMC has a higher developed land use which potentially increased nitrate levels and a higher agricultural land use that likely contributed to the elevated chloride levels compared to MC.

Storm flow accounted for almost all suspended sediment loading and the entire nutrient loading on SMC and MC indicating the importance of large storm event data collection. The dynamic discharge and hysteresis patterns generated by storm events were due to temporal variations in sediment availability and stream transport capacity. By quantifying the sediment transport, and by understanding the internal mechanisms on each stream, we have begun to understand the unique characteristics that influence the sediment transport capacity of each stream in McLean County, IL.

REFERENCES

American Society for Testing and Materials (ASTM), 2000, Standard test methods for determining sediment concentration in water samples: D 3977-97, vol. 11.02, Water (II), p.395-400.

Ackerman, K. V., D. M. Mixon, E. T. Sundquist, R. F. Stallard, G. E. Schwarz, and D. W. Stewart (2009), RESIS—An updated version of the original Reservoir Sedimentation Survey Information System (RESIS) database, U.S. Geological. Survey, Data Ser., 434. (Available at http://pubs.usgs.gov/ds/ds434)

Alvarez-Cobelas, M., Angeler, D. G., & Sanchez-Carrillo, S., 2008, Export of nitrogen from catchments: a world-wide analysis, Environmental Pollution, v.156, no.2, p.261-269. doi:10.1016/j.envpol.2008.02.016.

Allen, P.M., Harmel, R.D., Dunbar, J.A., and Arnold, J.G., 2011, Upland contribution of sediment and runoff during extreme drought: A study of the 1947-1956 drought in the Blackland Prairie, Texas, Journal of Hydrology, v.407, p.1-11, doi: 10.1016/j.hydrol.2011.04.039.

Borah, D.K., Bera, M., and Shaw, S., 2003, Water, sediment, nutrient, and pesticide measurements in an agricultural watershed in Illinois during storm events, American Society of Agricultural Engineers, v.46, no.3, p.657-674, ISSN: 0001-1351.

Drewry,J.J., Newham, L.T.H., and Croke B.F.W., 2009, Suspended sediment, nitrogen and phosphorus concentrations and exports during storm-events to the Tuross estuary, Australia, Journal of Environmental Management, v.90, p.879–887, doi:10.1016/j.jenvmano.2008.02.004.

Eby, G.N., 2004. Principles of Environmental Geochemistry: Pacific Grove, CA, Brooks/Cole-Thomson Learning, p.193.

Evergreen Lake Watershed Planning Committee, Evergreen Lake Watershed Plan, 2008. Bloomington, IL.

Fraley, L. M., Miller, A. J. and Welty, C., 2009, Contribution of In-Channel Processes to Sediment Yield of an Urbanizing Watershed, Journal of the American Water Resources Association, v.45, p.748–766, doi: 10.1111/j.1752-1688.2009.00320.x.

Gao, P, and Josefson, M., 2012, Temporal variation of suspended sediment transport in Oneida Creek watershed, central New York, Journal of Hydrology, v.426-427, p.27-27, doi:10.1002/esp.2229.

Gillian, S., 2005, Diel turbidity fluctuations In stream in Gwinnett County, Georgia, in Proceedings of the 2005 Georgia Water Resources Conference, edited by Kathryn J. Hachter, Institute of Ecology, University of Georgia, Athens, Ga. http://www.gwri.gatech.edu/uploads/proceedings/2005/Gillaino.pdf

Graf, W.L., Wohl, E., Sinha, T., and Sabo, J.L., 2010, Sedimentation and sustainability of western American reservoirs, Water Resources Research, v.46, p.W12535, doi: 10.1029/2009WR008836.

Heritage, G.L. Van Niekerk, A.W., 1995, Drought conditions and sediment transport in the Sabie River, Koedoe: African Protected Area Conservation and Science, v.38, no.2, p.1-9. doi: 10.4102/koedoe.v38i2.311.

Huenemann T.W., Dibble, E.D., and Fleming, J.P., 2012, Influence of Turbidity on the Foraging of Largemouth Bass, Transactions of the American Fisheries Society, v.141, p.107-111, doi: 10.1080/00028487.2011.651554.

Haregeweyn, NO., Melesee, B., Tsunekawa, A., Tsubo, M., Meshesha, D., and Babulo Balana B. 2012, Reservoir sedimentation and its mitigating strategies: a case study of Angereb reservoir (NW Ethiopia), Journal of Soil Sediments, v.12, p.291-305, doi: 10.1007/s11368-011-0447-z.

Hudson, P.F., 2003, Event sequence and sediment exhaustion in the lower Panuco basin, Mexico, Catena, v.52, no.1, p.57-59, doi: 10.1016/S0341-8162(02)00145-5.

ISGS, 2012, Illinois State Climatologist, Illinois State Water Survey: August Near-Normal But Summer Hot, Dry for Illinois, http://climateillinois.wordpress.com/ (September 2012).

Kennedy, C.D., 2012, Batialle, C., Liu, Z.F., Ale, S., VanDeVelde, L., Rosewell, C.R., Bowling, L.C., Bowen, G.J., Dynamics of nitrate and chloride during storm events in agricultural catchments with different subsurface drainage intensity (Indiana, USA): Journal of Hydrology, v.466, p.1-10, doi: 10.1016/j.jhydrol.2012.05.002.

Kinney, W., 2006, Assessment of Sediment Delivery and Stream Conditions in the Lake Bloomington Watershed, Bloomington Water Purification Plant. Bloomington, IL.

Kinney, W., 2005, Assessment of Sediment Delivery and Stream Conditions in the Evergreen Lake Watershed, Bloomington Water Purification Plant. Bloomington, IL.

Kovacic, D.A., Twait R.M., Wallace, M.P., and Bowling, J. M., 2006, Use of created wetlands to improve water quality in the Midwest-Lake Bloomington case study, Ecological Engineering, v.28, p.258-270, doi: 10.1016/j.ecoleng.2006.08.002.

Khanchoul, K., Boukhrissa, Z.E., Acidi, A., Altschul, R., 2012, Estimation of suspended sediment transport in the Kebir drainage basin, Algeria, Quaternary International, v.262, p.25-31, doi: 10.1016/j.quaint.2010.08.016.

Lake Bloomington Watershed Plan, Lake Bloomington Watershed Planning Committee, June 22, 2008. Bloomington, IL.

Lax S, and Peterson, E.W.,2009, Characterization of chloride transport in the unsaturated zone near salted road, Environmental Geology, v. 58, p.1041-1049, doi:1010.1007/s00254-00008-01584-00256. doi:10.1007/s00254-008-1584-6.

Lecce, S.A., Pease, P.A., Gares, P.A., and Wang, J., 2005, Seasonal controls on sediment delivery in a small coastal plain watershed, North Carolina, USA, Geomorphology, v.73, p. 246-260, doi:10.1016.j.geomorph.2005.05.017.

Lefranchois, J., Grimaldi, C., Gascuel-Odoux, C., and Gilliet, N., 2007, Suspended sediment and discharge relationships to identify bank degradation as a main sediment source on small agricultural catchments, Hydrological Processes, v.21, p.2923-2933, doi: 10.1002/hyp.6509.

Lenzi, M.A., Lorenzo, M., 2000, Suspended sediment load during floods in a small stream of the Dolomites (northeastern Italy), Catena, v.39, no.4, p.267-282, doi: 10.1016/S0341-8162(00)00079-5.

Ludwig, W. and Probst, J.L., 1998, River sediment discharge to the oceans; present-day controls and global budgets, American Journal of Science, v.298, p.265-295, doi: 10.2475/ajs.298.4.265.

Loperfido, J. V., Just, C.L., Papanicolaou, A.N., and Schnoor, J.L., 2010, In situ sensing to understand diel turbidity cycles, suspended solids, and nutrient transport in Clear Creek, Iowa, Water Resources Research, v.46, p.1-8, doi: 10.1029/2009WR008293.

Miller, J.D., Schoonover, J.E., Williard, K.W.J., Hwang, C.R., Whole Catchment Land Cover Effects on Water Quality in the Lower Kaskaskia River Watershed, 2011, Water Air Soil Pollution, v.221, p.337-350, doi:10.1007/s11270-011-0794-9.

Mosley, M.P. and Mckerchar, A.I. (1993) Streamflow. Handbook of Hydrology (ed D.R. Maidment), pp.8.1-8.39. McGraw Hill, New York.

Outiero, L., Ubeda, X., and Farguell, J., 2010, The impact of agriculture of solute and suspended sediment load on a Mediterranean watershed after intense rainstorms, Earth Surface Processes and Landforms, v.35, p.549-560, doi:10.1002/esp.1943.

Pelletier, J.D., 2012, A spatially distributed model for the long-term suspended sediment discharge and delivery ratio of drainage basins, Journal of Geophyiscal Research, v.117, p.1-15, doi:10.1029/2011JF002129.

Peterson, E.W., Sickbert, T.B., and Moore S.L., 2008, High frequency stream bed mobility of a low-gradient agricultural stream with implications on the hyporheic zone, Hydrological Processes, v 22, p.4239-4248, doi:10.1002/hyp.7031.

Restrepo, J.D., Kjerfve, B., Hermelin, M., and Restrepo, J.C., 2006, Factors controlling sediment yield in a major South American drainage basin: The Magdalena River, Colombia, Journal or Hydrology, v.316, p.213-232, doi:10.1016/j.hydrol.2005.05.002.

Royer, T.V., David, M.B., and Gentry, L.E., 2006, Timing of Riverine Export of Nitrate and Phosphorus from Agricultural Watersheds in Illinois: Implications for Reducing Nutrient Loading to the Mississippi River, Environmental Science and Technology, v.40, no.40,p.4126-4131, doi:10.102/es052573n.

Salant, NO.L, Hassan, M.A., and Alonso, C.V., 2008, Suspended sediment dynamics at high and low storm flows in two small catchments: Hydrological Processes, v.22, p.1573-1587, doi:10.1002/hyp.6743.

Skaggs, R.W., Breve, M.A., Gilliam, J.W., 1994, Hydrologic and water-quality impacts of agricultural drainage: Critical Reviews in Environmental Science and Technology, v.24, no.1, p.1-32.

Soil Survey of McLean County, Illinois, 2002, United States Department of Agriculture & Natural Resources Conservation Services, http://soildatamart.nrcs.usda.gov/Manuscripts/IL113/0/McLean_IL.pdf.

Smith, H.G., 2009, Estimation of suspended sediment loads and delivery in an incised upland headwater catchment, south-eastern Australia, Hydrological Processes, v.22, p.3135-3148, doi:10.1002/hyp.6898.

Smith, H.G., and Dragovich, D., 2009, Interpreting sediment delivery processes using suspended sediment-discharge hysteresis patterns from nested upland catchments, south-eastern Australia, Hydrological Processes, v. 23, p. 2415-2425, doi:10.1002/hyp.7357.

Sutherland, A.B. and Meyer, J.L., 2007, Effects of increased suspended sediment on growth rate and gill condition of two southern Appalachian minnows, Environmental Biology of Fishes, v.80, p.389–403, doi: 10.1007/s10641-006-9139-8.

Trimble, S. W. 1999, Decreased rates of alluvial sediment storage in the Coon Creek basin, Wisconsin, USA, 1975-1993, Science, v.285, p.1244-1246.

U.S. Environmental Protection Agency, 2009, List of Contaminants & their MCLs. EPA: 816-F-09-0004.

U.S. Environmental Protection Agency, 2000, The Quality of Our Nation's Waters, A Summary of the National Water Quality Inventory: 1998 Report to Congress, Office of Water, 841-S-00-001, Washington, D.C.

U.S. Environmental Protection Agency, 1998, Report of the Federal Advisory Committee on the Total Maximum Daily Load (TMDL) Program: The National Advisory Council for Environmental Policy and Technology, EPA 100-R-98-006, 97 p., 7 appendices.

Vache, K.B., Eilers, J.M., and Santelmann, M.V., 2002, Water quality modeling of alternative agricultural scenarios in the US corn belt, Journal of the American Water Resources Association, v.38, no.3, p.773-787.

Van der Hoven, S. J., Froom, N.J., and Peterson, E.W., 2008, Quantifying nitrogen cycling beneath a meander of a low gradient, N-impacted, agricultural stream using tracers and numerical modeling, Hydrological Processes, v. 22, no. 8, p. 1206-1215, doi: 10.1002/hyo.6691.

Williams, G.P., 1989, Sediment concentration versus water discharge during single hydrologic events, Journal of Hydrology, v. 111, p.89–106.

Woodhouse, C.A., and Overpeck, J.T., 1998, 2000 years of drought variability in the central United States, Bulletin of the American Meteorological Society, v.79, p.2693-2714.

World Health Organization (WHO), 2004, Sulfate in Drinking-water, Background document for development of WHO Guidelines for Drinking-water Quality.

APPENDIX A

SIGMA 900 MAX INSTRMENTATION STORM EVENT SET-UP

Sigma 900 Max Program Set-up		
Sample #	Time interval (minute)	Time interval (hour)
1	1	0.02
2	5	0.08
3	15	0.25
4	30	0.5
5	30	0.5
6	60	1
7	60	1
8	60	1
9	60	1
10	60	1
11	60	1
12	60	1
13	60	1
14	60	1
15	120	2
16	120	2
17	120	2
18	120	2
19	120	2
20	120	2
21	120	2
22	120	2
23	120	2
24	2619	43.65
Total time	4320	72

APPENDIX B

BASEFLOW STATISTICS

Baseflow Statistics		
Discharge	t(17) = -1.15, p<0.266	m^3/s
Total suspended sediment	t(21) = -1.74, p<0.096	mg/L
Suspended sediment load	t (17) = -0.11, p<0.915	mg/s
Suspended sediment load/drainage area	t(17) = 0.63, p<0.533	kg/m^2s

APPENDIX C

BASEFLOW DATA CALCULATIONS FOR SIX MILE CREEK AND MONEY CREEK

DATE	Stream	Stage (ft)	Stage (m)	Discharge (ft^3/s)	Discharge (m^3/s)	Organic SS (mg/L)	Inorganic SS (mg/L)	Total SS (mg/L)	% Organic	% Inorganic	Turbidity (NTU)	Load (mg/s)	TSS load/drainage area (kg/m^2s)
7/25	SMC	0.63	0.19	0.25	0.01	12.50	5.00	17.50	71.43	28.57	5.06	123	3
8/5	SMC	0.64	0.20	0.25	0.01	1.50	6.00	7.50	20.00	80.00	4.59	53	1
8/24	SMC	0.63	0.19	0.25	0.01	0.88	4.12	5.00	11.48	88.52	7.35	35	1
8/28	SMC	0.66	0.20	0.42	0.01	4.77	36.77	41.54	8.00	92.00	91.00	489	10
9/21	SMC	0.76	0.23	0.46	0.01	0.61	2.42	3.03	20.00	80.00	3.75	39	1
11/1	SMC	1.12	0.34	1.82	0.05	1.13	2.63	3.75	30.00	70.00	7.24	193	4
11/7	SMC	1.17	0.36	1.49	0.04	0.99	2.73	3.84	25.88	71.17	3.84	162	3
11/29	SMC	1.02	0.31	0.58	0.02	2.75	12.25	15.00	18.33	81.67	4.89	247	5
12/12	SMC	1.00	0.30	0.69	0.02	1.00	2.75	3.75	26.67	73.33	5.73	73	2
3/21	SMC	1.82	0.55	13.93	0.39	2.63	13.63	16.25	16.15	83.85	13.00	6404	135
7/25	MC	0.23	0.07	0.11	0.00	4.00	7.67	12.00	33.33	63.89	11.30	36	0
8/5	MC	n.a.	n.a.	n.a.	n.a.	23.56	65.33	89.00	26.47	73.41	129.00	n.a.	n.a.
8/24	MC	0.46	0.14	0.42	0.01	1.87	4.80	7.00	26.67	68.57	9.45	84	1
8/28	MC	0.52	0.16	0.95	0.03	8.22	21.92	30.00	27.40	73.06	30.10	810	7
9/21	MC	0.46	0.14	0.71	0.02	1.71	7.50	9.00	19.01	83.33	n.a.	180	2
11/1	MC	1.26	0.38	12.38	0.35	1.20	5.80	7.00	17.14	82.86	7.03	2453	22
11/7	MC	1.08	0.33	5.36	0.15	1.37	6.09	7.00	19.52	86.96	6.49	1063	9
11/29	MC	0.76	0.23	2.00	0.06	1.13	2.63	4.00	28.12	65.63	16.40	226	2
12/12	MC	0.84	0.26	4.72	0.13	2.27	17.59	20.00	11.35	87.94	21.10	2669	24
3/21	MC	1.67	0.51	14.08	0.40	12.40	58.46	71.00	17.47	82.34	10.00	226	0
Average on SMC		0.94	0.29	2.01	0.06	2.87	8.83	11.70	24.56	75.44	14.65	782	17
Average on MC		0.81	0.25	4.53	0.13	5.77	19.78	25.55	22.59	77.41	26.76	861	7.4

APPENDIX D

SIX MILE CREEK BASEFLOW AND STORM FLOW TOTAL NITRATE LOAD/TIME STEP

Six Mile Creek NO_3-N Load			
Baseflow	Date	Suspended sediment load/time step (kg)	% Suspended Sediment load/event
Baseflow 1	Jul.3-Aug.16	6.48E-04	0.00
Baseflow 2	Aug.17-Sept.1	2.23E-04	0.00
Baseflow 3	Sept.2-Oct.5	4.88E-04	0.00
Baseflow 4	Oct.5-13	1.00E-04	0.00
Baseflow 5	Oct.17	1.95E-05	0.00
Baseflow 6	Oct.21-26	7.07E-05	0.00
Baseflow 7	Oct.29-Nov.12	1.95E-04	0.00
Baseflow 8	Nov.12-Dec.2	3.03E-04	0.00
Baseflow 9	Dec.5-Jan.29	7.67E-04	0.00
Baseflow 10	Jan.31-Feb.10	1.47E-04	0.00
Baseflow 11	Feb.12-26	2.05E-04	0.00
Baseflow 12	Feb.28-Mar.1	1.98E-05	0.00
STORM EVENTS	Date	load per storm/time step (kg)	% Suspended Sediment load/event
Event 1	Aug.16-17	5.7	0.04
Event 2	Sept.1-4	22.7	0.17
Event 3	Oct.5-6	2.8	0.02
Event 4	Oct.13-17	15.8	0.12
Event 5	Oct.17-21	9.1	0.07
Event 6	Oct.26-29	68.5	0.50
Event 7	Nov.9-12	57.0	0.42
Event 8	Dec.2-6	18.7	0.14
Event 9	Jan.29-31	8.41E+03	61.66
Event 10	Feb.10-12	1.07E+03	7.87
Event 11	Feb.26-28	5.71E+02	4.19
Event 12	Mar.10-12	3.38E+03	24.81
Total BASEFLOW NO_3-N load		3.19E-03	kg/yr
Total STORM FLOW NO_3-N load		1.36E+04	kg/yr
TOTAL NO_3-N LOAD		1.36E+04	kg/yr
TOTAL NO_3-N LOAD/DRAINAGE AREA		289	kg/km^2
% Baseflow NO_3-N load		0.00	%
% Storm flow NO_3-N load		100.00	%

APPENDIX E

SIX MILE CREEK BASEFLOW AND STORM FLOW TOTAL CHLORIDE LOAD/TIME STEP

Six Mile Creek Cl^- Load			
Baseflow	Date	Suspended sediment load/time step (kg)	% Suspended Sediment load/event
Baseflow 1	Jul.3-Aug.16	1.13E-02	0.00
Baseflow 2	Aug.17-Sept.1	3.87E-03	0.00
Baseflow 3	Sept.2-Oct.5	8.49E-03	0.00
Baseflow 4	Oct.5-13	1.74E-03	0.00
Baseflow 5	Oct.17	3.40E-04	0.00
Baseflow 6	Oct.21-26	1.23E-03	0.00
Baseflow 7	Oct.29-Nov.12	3.39E-03	0.00
Baseflow 8	Nov.12-Dec.2	5.27E-03	0.00
Baseflow 9	Dec.5-Jan.29	1.34E-02	0.00
Baseflow 10	Jan.31-Feb.10	2.56E-03	0.00
Baseflow 11	Feb.12-26	3.57E-03	0.00
Baseflow 12	Feb.28-Mar.1	3.44E-04	0.00
STORM EVENTS	Date	load per storm/time step (g)	% Suspended Sediment load/event
Event 1	Aug.16-17	188.1	0.13
Event 2	Sept.1-4	2.49E+03	1.75
Event 3	Oct.5-6	2.01E+02	0.14
Event 4	Oct.13-17	1.59E+03	1.12
Event 5	Oct.17-21	1.50E+03	1.05
Event 6	Oct.26-29	1.53E+03	1.07
Event 7	Nov.9-12	2.37E+03	1.67
Event 8	Dec.2-6	7.19E+02	0.51
Event 9	Jan.29-31	1.10E+05	77.57
Event 10	Feb.10-12	8.64E+02	0.61
Event 11	Feb.26-28	5.68E+03	3.99
Event 12	Mar.10-12	1.48E+04	10.40
Total BASEFLOW Cl^- load		5.54E-02	kg/yr
Total STORM FLOW Cl^- load		1.42E+05	kg/yr
TOTAL Cl^- LOAD		1.42E+05	kg/yr
TOTAL Cl^- LOAD/DRAINAGE AREA		3012	kg/km²
% Baseflow Cl^- load		0.00	%
% Storm flow Cl^- load		100.00	%

Shaded grey cells had some areas under the curve for chloride concentration calculations that were below the lowest standard curve value of 7.267 µS*min. Low chloride areas ranged from 2.765-6.363 µS*min.

APPENDIX F

MONEY CREEK BASEFLOW AND STORM FLOW TOTAL NITRATE LOAD/TIME STEP

Money Creek NO_3-N Load			
Baseflow	Date	Suspended sediment load/time step (kg)	% Suspended Sediment load/event
Baseflow 1	Jul.3-Aug.16	1.74E-03	0.00
Baseflow 2	Aug.17-Sept.1	5.98E-04	0.00
Baseflow 3	Sept.2-Oct.5	1.31E-03	0.00
Baseflow 4	Oct.5-13	2.69E-04	0.00
Baseflow 5	Oct.17	5.25E-05	0.00
Baseflow 6	Oct.21-26	1.90E-04	0.00
Baseflow 7	Oct.29-Nov.12	5.24E-04	0.00
Baseflow 8	Nov.12-Dec.2	8.14E-04	0.00
Baseflow 9	Dec.5-Jan.29	2.06E-03	0.00
Baseflow 10	Jan.31-Feb.10	3.95E-04	0.00
Baseflow 11	Feb.12-26	5.52E-04	0.00
Baseflow 12	Feb.28-Mar.1	5.31E-05	0.00
STORM EVENTS	Date	Suspended sediment load per storm/time step (kg)	% Suspended Sediment load/event
Event 1	Aug.16-17	b.d.	b.d.
Event 2	Sept.1-4	4.83E+02	2.63
Event 3	Oct.5-6	63.6	0.35
Event 4	Oct.13-17	5.22E+03	n.a.
Event 5	Oct.17-21	n.a.	n.a.
Event 6	Oct.26-29	5.95E+03	32.40
Event 7	Nov.9-12	1.63E+03	8.85
Event 8	Dec.2-6	4.96E+02	2.70
Event 9	Jan.29-31	n.a.	n.a.
Event 10	Feb.10-12	n.a.	n.a.
Event 11	Feb.26-28	4.53E+03	24.68
Event 12	Mar.10-12	n.a.	n.a.
Total BASEFLOW NO_3-N load		8.56E-03	kg/yr
Total STORM FLOW NO_3-N load		1.84E+04	kg/yr
TOTAL NO_3-N LOAD		1.84E+04	kg/yr
TOTAL NO_3-N LOAD/DRAINAGE AREA		163	kg/m^2
% Baseflow NO_3-N load		0.00	%
% Storm flow NO_3-N load		100.00	%

APPENDIX G

MONEY CREEK BASEFLOW AND STORM FLOW TOTAL CHLORIDE LOAD/TIME STEP

Money Creek Cl^- Load			
Baseflow	Date	Suspended sediment load/time step (kg)	% Suspended Sediment load/event
Baseflow 1	Jul.3-Aug.16	2.63E-02	0.00
Baseflow 2	Aug.17-Sept.1	9.03E-03	0.00
Baseflow 3	Sept.2-Oct.5	1.98E-02	0.00
Baseflow 4	Oct.5-13	4.05E-03	0.00
Baseflow 5	Oct.17	7.93E-04	0.00
Baseflow 6	Oct.21-26	2.87E-03	0.00
Baseflow 7	Oct.29-Nov.12	7.91E-03	0.00
Baseflow 8	Nov.12-Dec.2	1.23E-02	0.00
Baseflow 9	Dec.5-Jan.29	3.11E-02	0.00
Baseflow 10	Jan.31-Feb.10	5.96E-03	0.00
Baseflow 11	Feb.12-26	8.33E-03	0.00
Baseflow 12	Feb.28-Mar.1	8.01E-04	0.00
STORM EVENTS	Date	Suspended sediment load per storm/time step (kg)	% Suspended Sediment load/event
Event 1	Aug.16-17	57	0.23
Event 2	Sept.1-4	1.32E+04	53.73
Event 3	Oct.5-6	1.73E+02	0.71
Event 4	Oct.13-17	n.a.	n.a.
Event 5	Oct.17-21	n.a.	n.a.
Event 6	Oct.26-29	7.79E+03	31.84
Event 7	Nov.9-12	1.49E+03	6.10
Event 8	Dec.2-6	7.27E+02	2.97
Event 9	Jan.29-31	n.a.	n.a.
Event 10	Feb.10-12	n.a.	n.a.
Event 11	Feb.26-28	1.08E+03	4.41
Event 12	Mar.10-12	n.a.	n.a.
Total BASEFLOW Cl^- load		0	kg/yr
Total STORM FLOW Cl^- load		2.45E+04	kg/yr
TOTAL Cl^- LOAD		2.45E+04	kg/yr
TOTAL Cl^- LOAD/DRAINAGE AREA		217	kg/km²
% Baseflow Cl^- load		0.00	%
% Storm flow Cl^- load		100.00	%

Shaded grey cell had some areas under the curve for chloride concentration calculations that were below the lowest standard curve value of 7.187 µS*min. Low chloride areas ranged from 3.295-6.591 µS*min.

APPENDIX H

SIX MILE CREEK STORM BASEFLOW AND STORM FLOW TOTAL SUSPENDED SEDIMENT

LOAD/TIME STEP

Six Mile Creek TSS Load			
Baseflow	Period	Suspended sediment load/time step (kg)	% Suspended Sediment load/event
Baseflow 1	Jul.3-Aug.16	50	0.05
Baseflow 2	Aug.17-Sept.1	17	0.02
Baseflow 3	Sept.2-Oct.5	38	0.04
Baseflow 4	Oct.5-13	8	0.01
Baseflow 5	Oct.17	2	0.00
Baseflow 6	Oct.21-26	5	0.01
Baseflow 7	Oct.29-Nov.12	15	0.01
Baseflow 8	Nov.12-Dec.2	23	0.02
Baseflow 9	Dec.5-Jan.29	59	0.06
Baseflow 10	Jan.31-Feb.10	11	0.01
Baseflow 11	Feb.12-26	16	0.02
Baseflow 12	Feb.28-Mar.1	2	0.00
STORM EVENTS	Period	Suspended sediment load per storm/time step (kg)	% Suspended Sediment load/event
Event 1	Aug.16-17	7	0.01
Event 2	Sept.1-4	213	0.21
Event 3	Oct.5-6	2	0.00
Event 4	Oct.13-17	19	0.02
Event 5	Oct.17-21	12	0.01
Event 6	Oct.26-29	13	0.01
Event 7	Nov.9-12	7	0.01
Event 8	Dec.2-6	5	0.00
Event 9	Jan.29-31	2.93E+04	28.33
Event 10	Feb.10-12	442	0.43
Event 11	Feb.26-28	88	0.09
Event 12	Mar.10-12	7.30E+04	70.65
Total BASEFLOW SS		246	kg/yr
Total STORM FLOW SS		1.03E+05	kg/yr
TOTAL SUSPENDED SEDIMENT		1.03E+05	kg/yr
TOTAL SUSPENDED SEDIMENT LOAD/DRAINAGE AREA		2185	kg/km²
Baseflow TSS LOAD		0.24	%
Storm flow TSS LOAD		99.76	%

APPENDIX I

MONEY CREEK STORM BASEFLOW AND STORM FLOW TOTAL SUSPENDED SEDIMENT

LOAD/TIME STEP

Money Creek TSS Load			
Baseflow	Period	Suspended sediment load per storm/time step (kg)	% Suspended Sediment load/event
Baseflow 1	Jul.3-Aug.16	43	1.07
Baseflow 2	Aug.17-Sept.1	18	0.45
Baseflow 3	Sept.2-Oct.5	39	0.96
Baseflow 4	Oct.5-13	7	0.19
Baseflow 5	Oct.17-26	11	0.28
Baseflow 6	Oct.26-Nov.12	13	0.33
Baseflow 7	Nov.12-Dec.2	24	0.60
Baseflow 8	Dec.5-Jan.29	68	1.70
Baseflow 9	Jan.31-Feb.26	32	0.80
Baseflow 10	Feb.26-Mar.1	9	0.22
STORM EVENTS	Period	Suspended sediment load per storm/time step (kg)	% Suspended Sediment load/event
Event 1	Aug.16-17	3	0.07
Event 2	Sept.1-4	898	22.35
Event 3	Oct.5-6	2	0.05
Event 4	Oct.13-17	213	5.30
Event 5	Oct.17-21	n.a	n.a
Event 6	Oct.26-29	2.05E+03	50.94
Event 7	Oct.9-12	34	0.83
Event 8	Dec.2-6	8	0.20
Event 9	Jan.29-31	453	11.27
Event 10	Feb.10-12	n.a	n.a
Event 11	Feb.26-28	96	2.39
Event 12	Mar.10-12	n.a	n.a
Total BASEFLOW SS		265	kg/yr
Total STORM FLOW SS		3.75E+03	kg/yr
TOTAL SUSPENDED SEDIMENT		4.02E+03	kg/yr
TOTAL SUSPENDED SEDIMENT LOAD/DRAINGE AREA		36	kg/km²
Baseflow TSS LOAD		6.60	%
Storm flow TSS LOAD		93.40	%

APPENDIX J

SIX MILE CREEK EVENT HYDROGRAPH, TSS, AND HYSTERESIS PATTERNS

EVENT 1

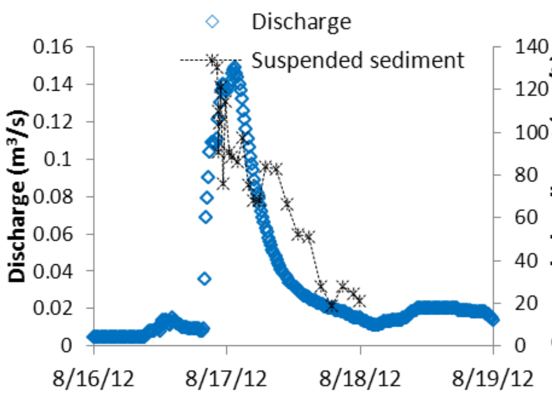

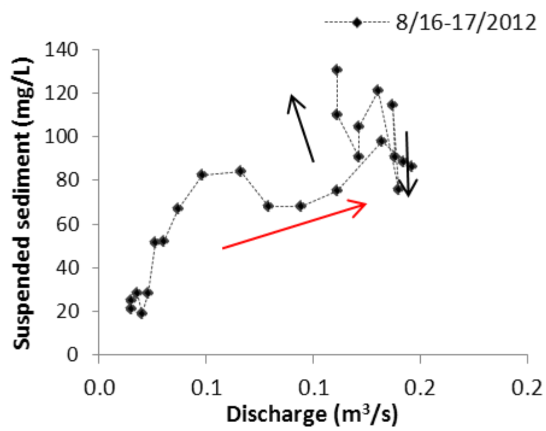

Six Mile Creek -Event 1	8/16-17/2012	Units
Average TSS per storm	74.1	mg/L
	0.08	m^3/s
Average Storm DISCHARGE	2.92	ft^3/s
	0.148	m^3/s
Peak Q	5.224	ft^3/s
Total Load per storm/time step	7	kg
Average sediment Flux	75.76	mg/s
Hysteresis pattern	random	

EVENT 2

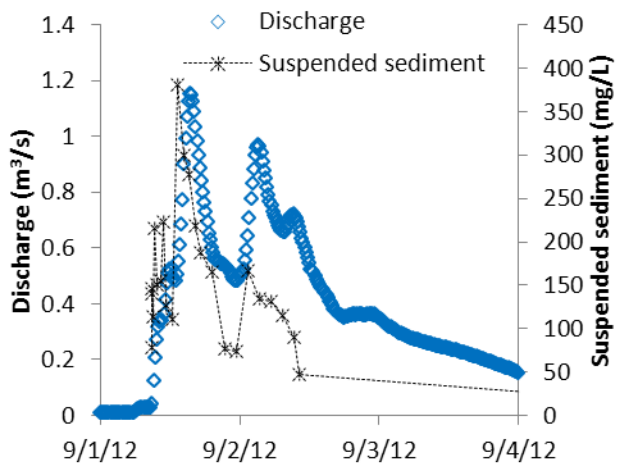

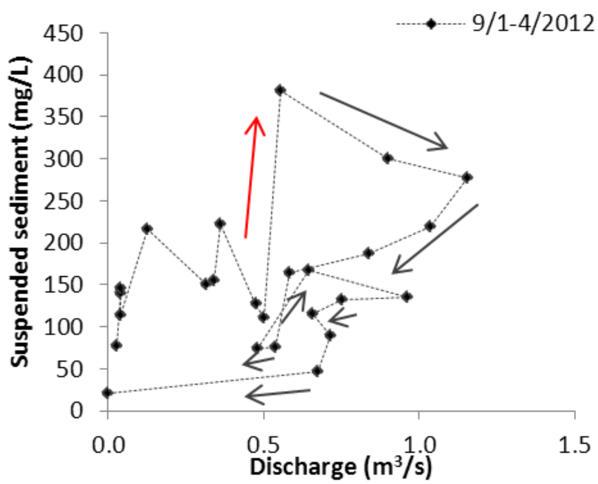

Six Mile Creek - Event 2	9/1-4/2012	Units
Average TSS per storm	153.9	mg/L
Average Storm DISCHARGE	0.53	m^3/s
	18.54	ft^3/s
Peak Q	1.154	m^3/s
	40.736	ft^3/s
Total Load per storm/time step	213	kg
Average sediment Flux	772.23	mg/s
Hysteresis pattern	double clockwise	

EVENT 3

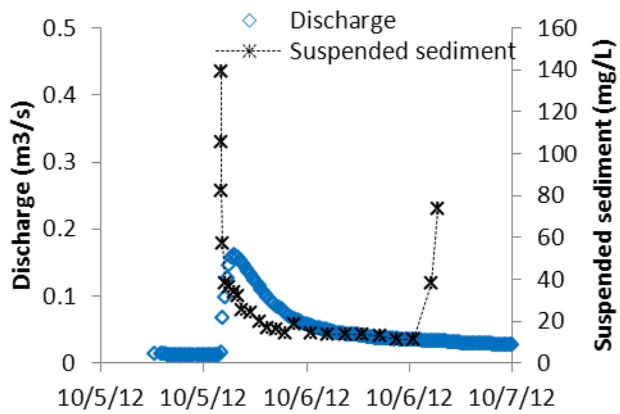

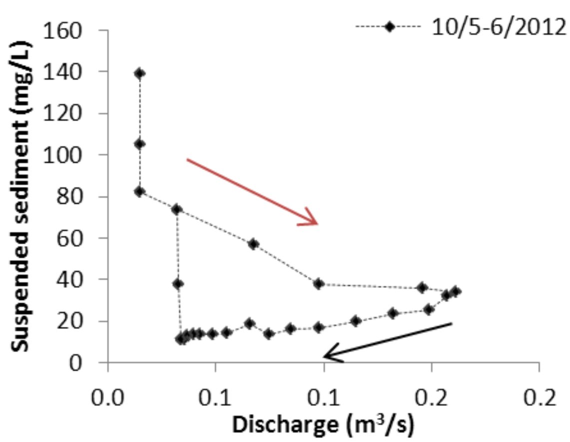

Six Mile Creek - Event 3	10/5-6/2012	Units
Average TSS per storm	35.8	mg/L
Average Storm DISCHARGE	0.07	m^3/s
	2.58	ft^3/s
Peak Q	0.157	m^3/s
	5.542	ft^3/s
Total Load per storm/time step	2	kg
Average sediment Flux	22.94	mg/s
Hysteresis pattern	clockwise	

EVENT 4

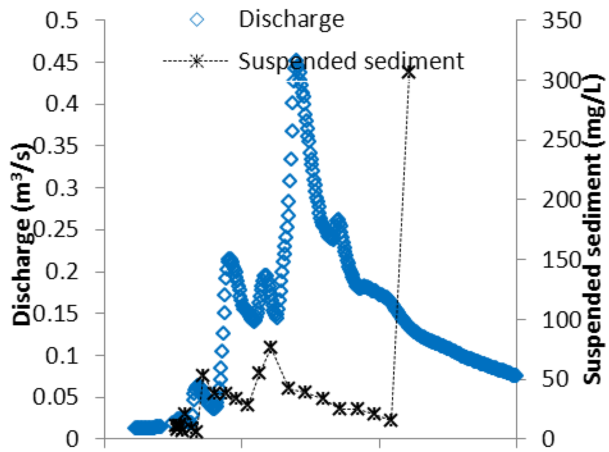

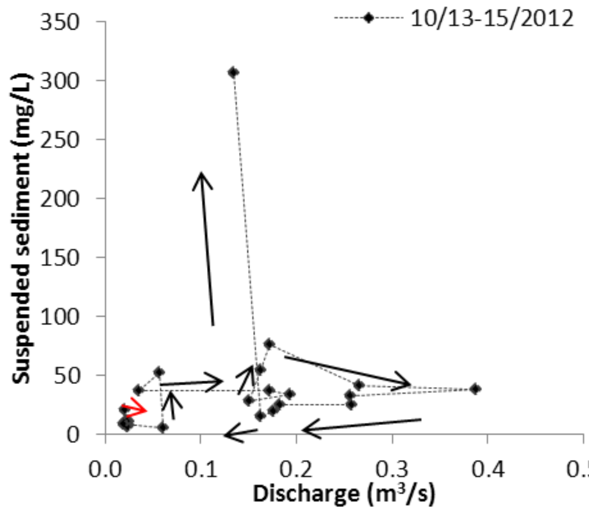

Six Mile Creek - Event 4	10/13-17/2012	Units
Average TSS per storm	39.7	mg/L
Average Storm DISCHARGE	0.13	m^3/s
	4.58	ft^3/s
Peak Q	0.452	m^3/s
	15.956	ft^3/s
Total Load per storm/time step	19	kg
Average sediment Flux	128.03	mg/s
Hysteresis pattern	random	

EVENT 5

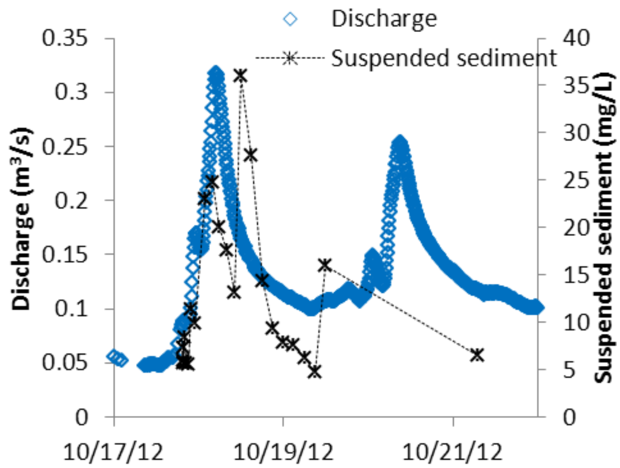

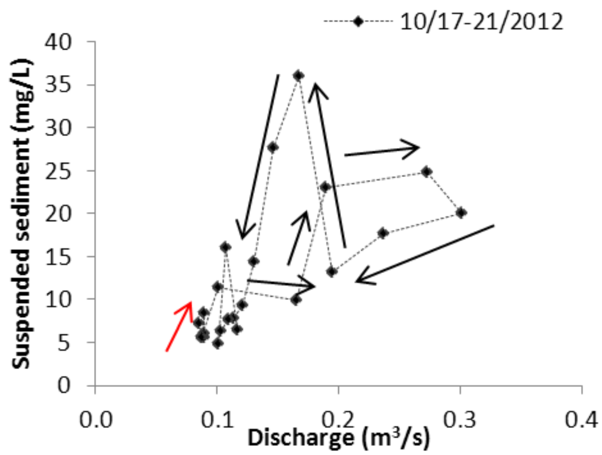

Six Mile Creek - Event 5	10/17-21/2012	Units
Average TSS per storm	15.6	mg/L
Average Storm DISCHARGE	0.14	m^3/s
	4.82	ft^3/s
Peak Q	0.312	m^3/s
	11.014	ft^3/s
Total Load per storm/time step	12	kg
Average sediment Flux	33.36	mg/s
Hysteresis pattern	random	

EVENT 6

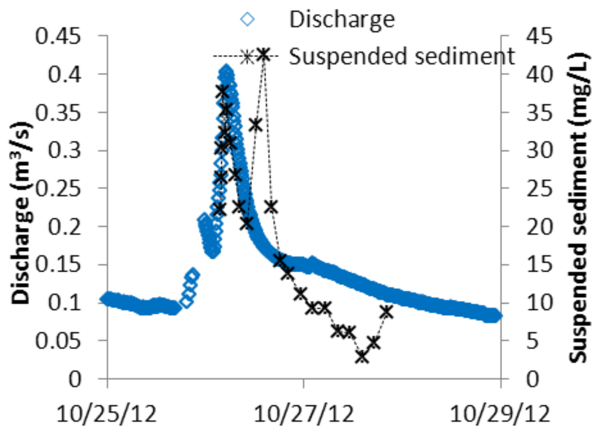

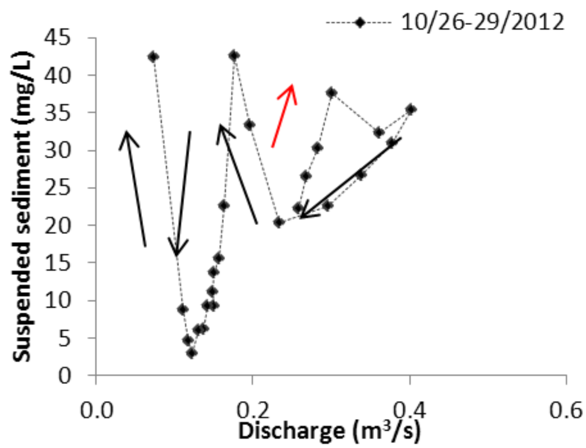

Six Mile Creek - Event 6	10/26-29/2002	Units
Average TSS per storm	21.4	mg/L
Average Storm DISCHARGE	0.21	m^3/s
	7.49	ft^3/s
Peak Q	0.403	m^3/s
	14.226	ft^3/s
Total Load per storm/time step	13	kg
Average sediment Flux	43.71	mg/s
Hysteresis pattern	random/clockwise	

EVENT 7

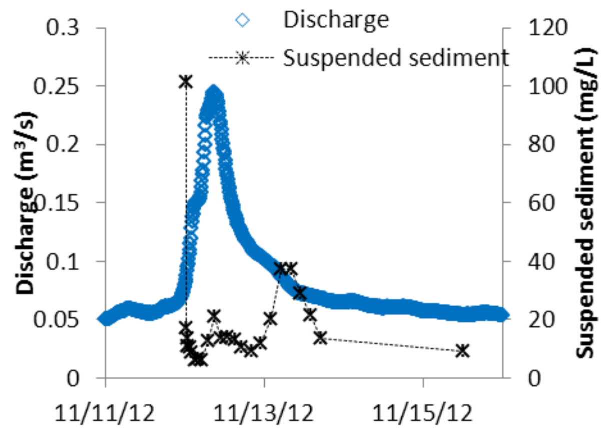

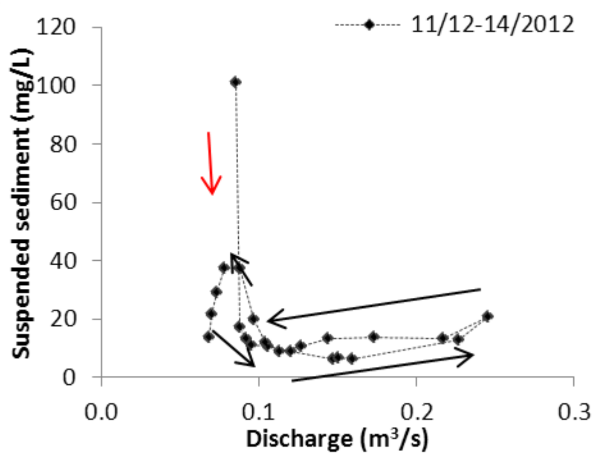

Six Mile Creek - Event 7	11/9-12/2012	Units
Average TSS per storm	19.0	mg/L
Average Storm DISCHARGE	0.08	m^3/s
	2.66	ft^3/s
Peak Q	0.243	m^3/s
	8.578	ft^3/s
Total Load per storm/time step	7	kg
Average sediment Flux	47.01	mg/s
Hysteresis pattern	counter-clockwise	

EVENT 8

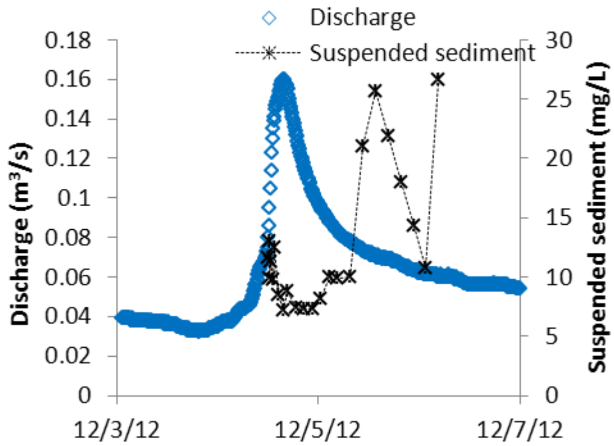

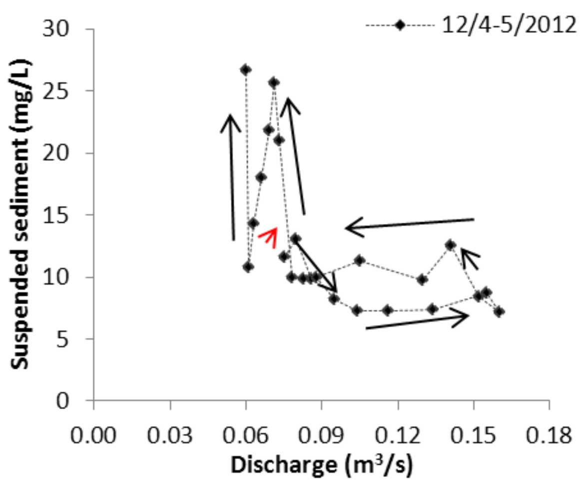

Six Mile Creek - Event 8	12/2-6/2012	Units
Average TSS per storm	12.6	mg/L
Average Storm DISCHARGE	0.10	m^3/s
	3.38	ft^3/s
Peak Q	0.160	m^3/s
	5.648	ft^3/s
Total Load per storm/time step	5	kg
Average sediment Flux	15.91	mg/s
Hysteresis pattern	random	

EVENT 9

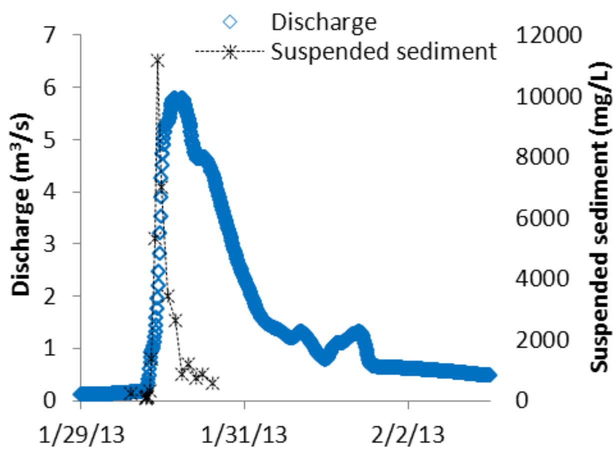

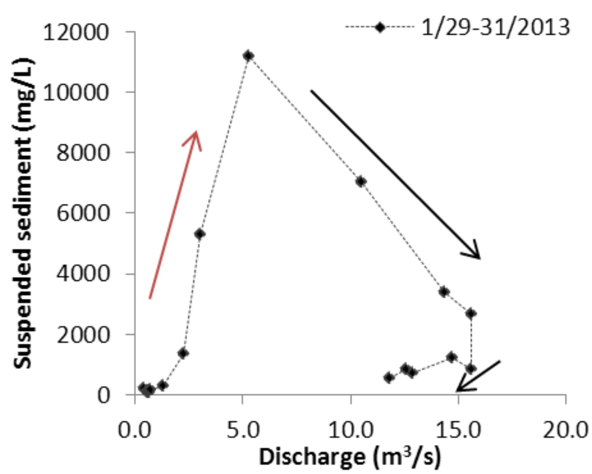

Six Mile Creek - Event 9	1/29-31/2013	Units
Average TSS per storm	2127.2	mg/L
Average Storm DISCHARGE	6.84	m^3/s
	241.44	ft^3/s
Peak Q	5.757	m^3/s
	203.222	ft^3/s
Total Load per storm/time step	29270	kg
Average sediment Flux	180013.88	mg/s
Hysteresis pattern	clockwise	

EVENT 10

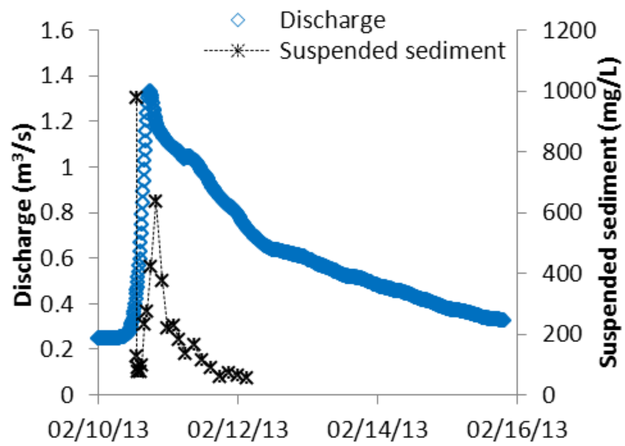

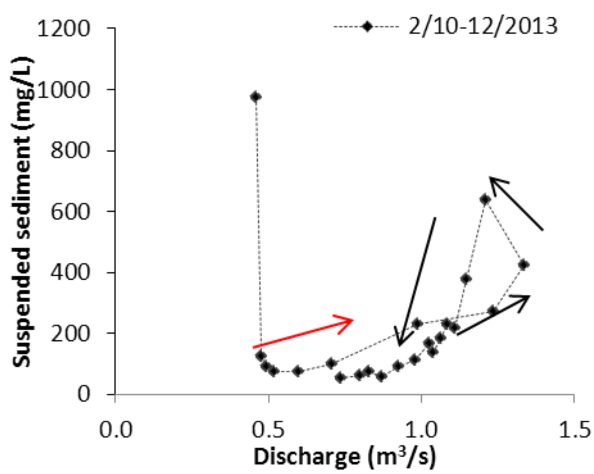

Six Mile Creek - Event 10	2/10-12/2013	Units
Average TSS per storm	230.9	mg/L
Average Storm DISCHARGE	0.87	m^3/s
	30.86	ft^3/s
Peak Q	1.334	m^3/s
	47.090	ft^3/s
Total Load per storm/time step	442	kg
Average sediment Flux	3030.94	mg/s
Hysteresis pattern	counter clockwise figure eight	

EVENT 11

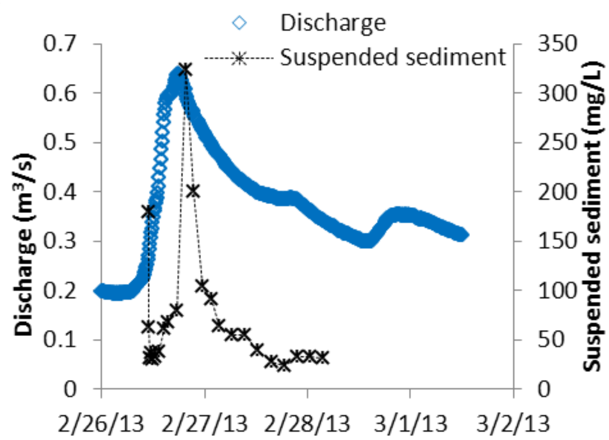

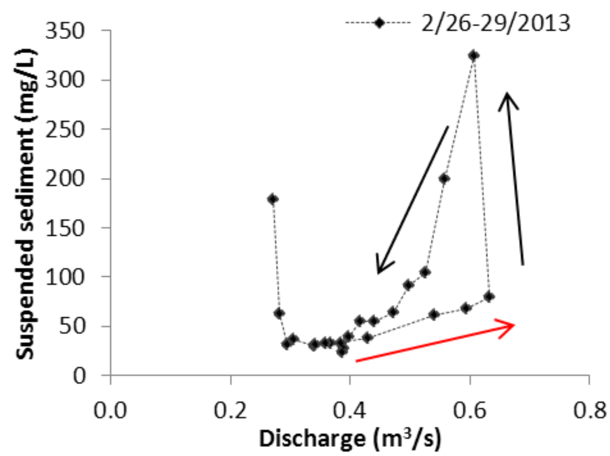

Six Mile Creek - Event 11	2/26-28/2013	Units
Average TSS per storm	73.9	mg/L
Average Storm DISCHARGE	0.43	m^3/s
	15.10	ft^3/s
Peak Q	0.636	m^3/s
	22.451	ft^3/s
Total Load per storm/time step	88	kg
Average sediment Flux	603.01	mg/s
Hysteresis pattern	counter clockwise figure eight	

EVENT 12

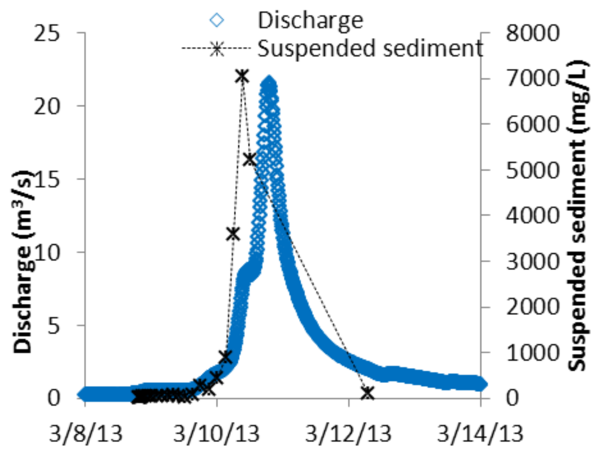

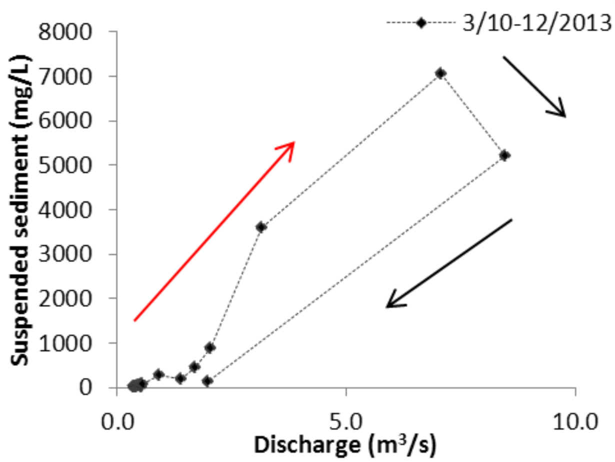

Six Mile Creek - Event 12	3/10-12/2013	Units
Average TSS per storm	769.5	mg/L
Average Storm DISCHARGE	1.43	m^3/s
	50.41	ft^3/s
Peak Q	21.348	m^3/s
	753.584	ft^3/s
Total Load per storm/time step	72983	kg
Average sediment Flux	242790.63	mg/s
Hysteresis pattern	clockwise	

APPENDIX K

MONEY CREEK EVENT HYDROGRAPH, TSS, AND HYSTERESIS PATTERNS

EVENT 1

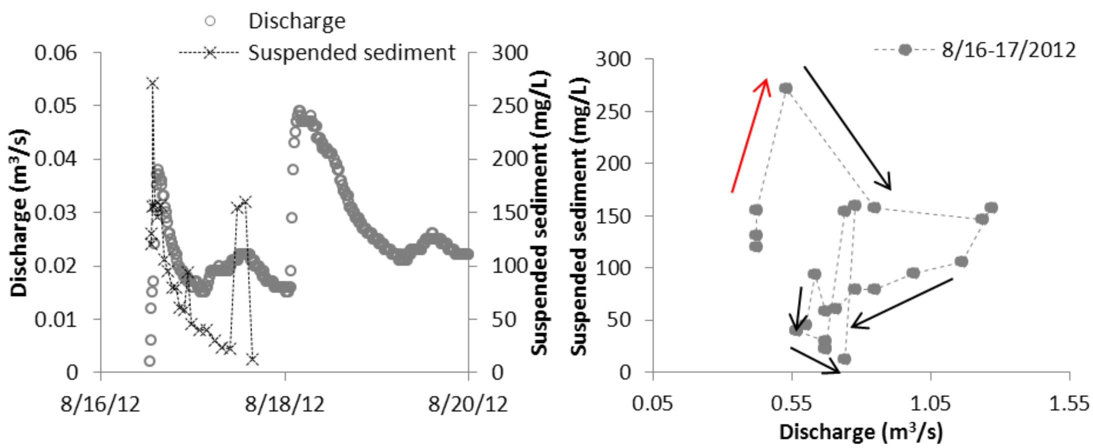

Money Creek -Event 1	8/16-17/2012	Units
Average TSS per storm	97.3	mg/L
Average Storm DISCHARGE	0.02	m^3/s
	0.74	ft^3/s
Peak Q	0.040	m^3/s
	1.412	ft^3/s
Total Load per storm/time step	3	kg
Average sediment Flux	30.04	mg/s
Hysteresis pattern	clockwise	

EVENT 2

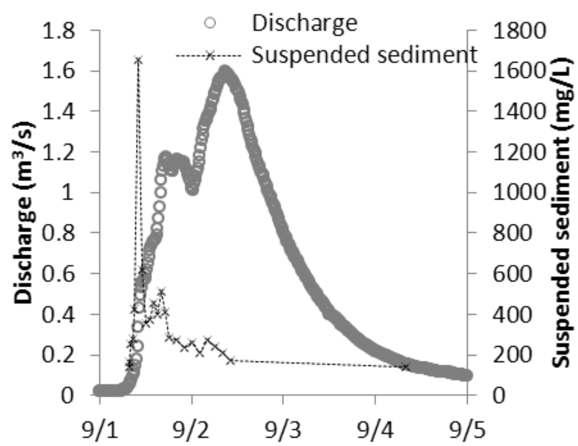

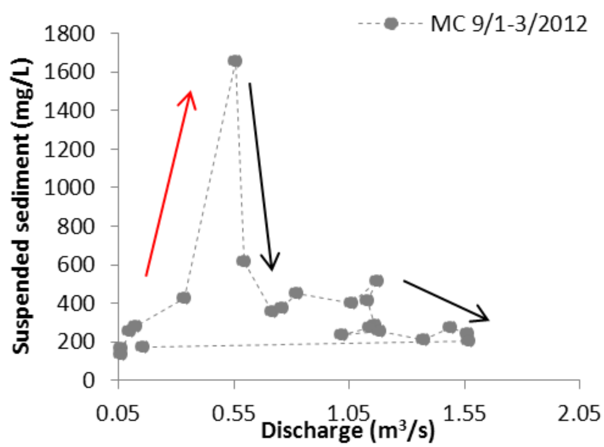

Money Creek - Event 2	9/1-4/2013	Units
Average TSS per storm	362.8	mg/L
Average Storm DISCHARGE	0.79	m^3/s
	27.90	ft^3/s
Peak Q	1.572	m^3/s
	55.492	ft^3/s
Total Load per storm/time step	898	kg
Average sediment Flux	3465.53	mg/s
Hysteresis pattern	clockwise	

EVENT 3

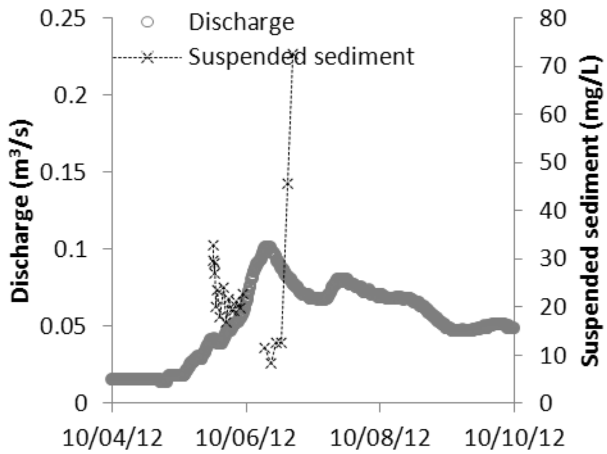

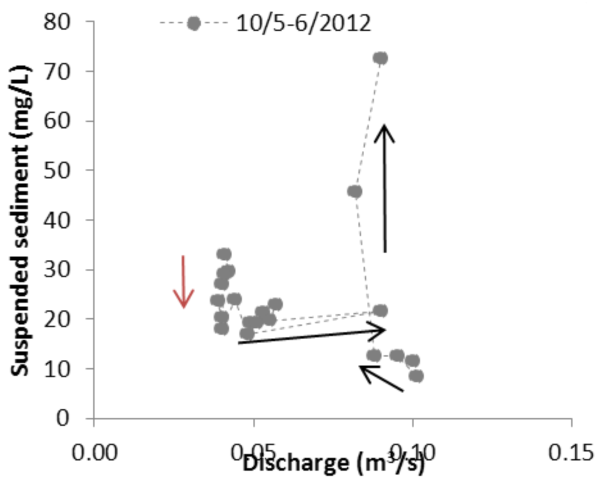

Money Creek - Event 3	10/5-6/2013	Units
Average TSS per storm	24.2	mg/L
	0.06	m^3/s
Average Storm DISCHARGE	2.25	ft^3/s
	0.105	m^3/s
Peak Q	3.707	ft^3/s
Total Load per storm/time step	2	kg
Average sediment Flux	19.17	mg/s
Hysteresis pattern	random	

EVENT 4

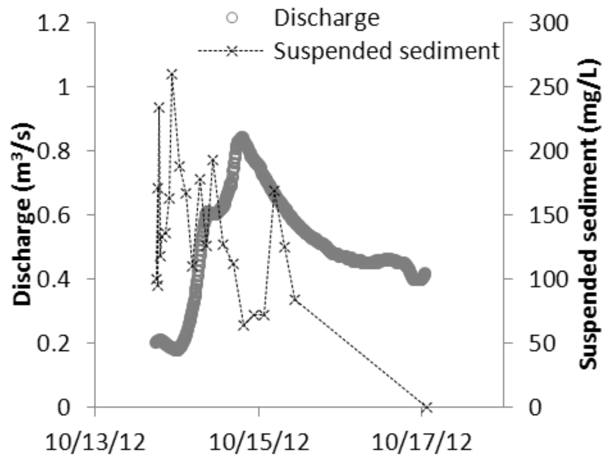

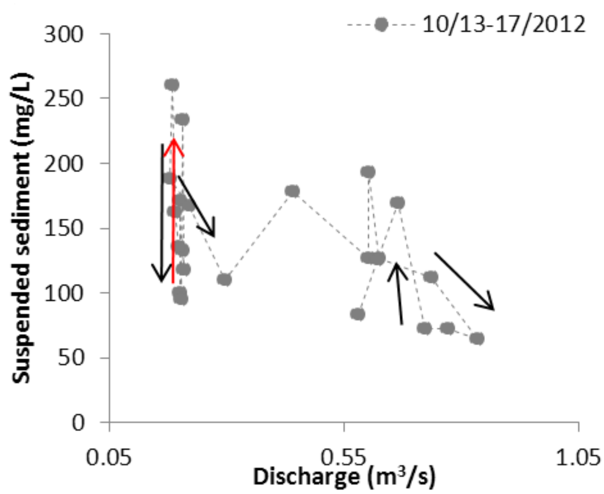

Money Creek - Event 4	10/13-17/2013	Units
Average TSS per storm	139.1	mg/L
Average Storm DISCHARGE	0.42	m^3/s
	14.86	ft^3/s
Peak Q		m^3/s
		ft^3/s
Total Load per storm/time step	213	kg
Average sediment Flux	746.47	mg/s
Hysteresis pattern	random	

EVENT 6

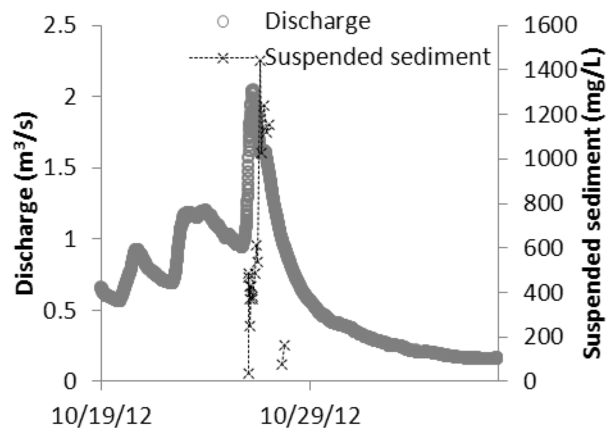

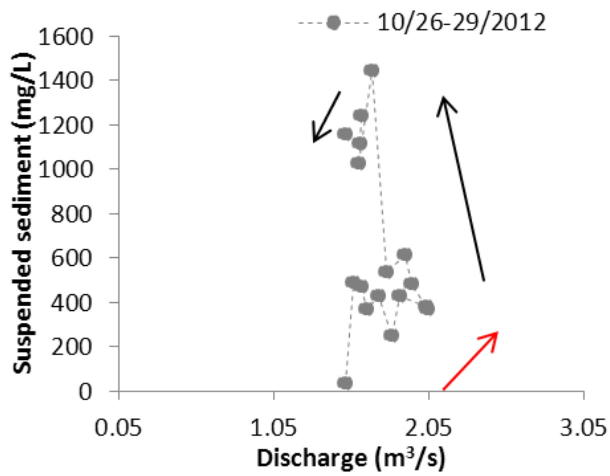

Money Creek - Event 6	10/26-29/2003	Units
Average TSS per storm	583.5	mg/L
Average Storm DISCHARGE	1.53	m^3/s
	54.15	ft^3/s
Peak Q	1.999	m^3/s
	70.565	ft^3/s
Total Load per storm/time step	2047	kg
Average sediment Flux	6769.49	mg/s
Hysteresis pattern	counter-clockwise	

EVENT 7

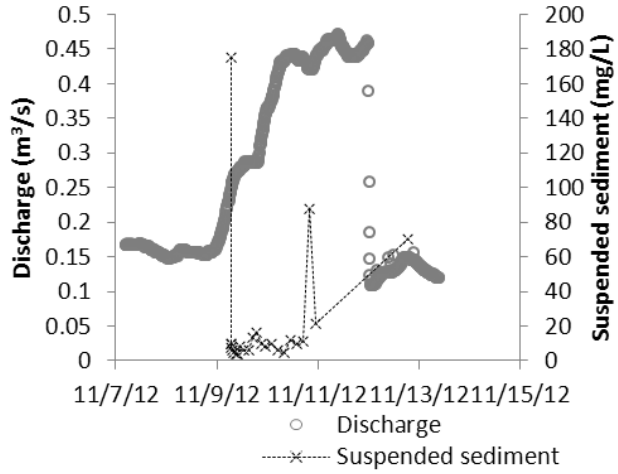

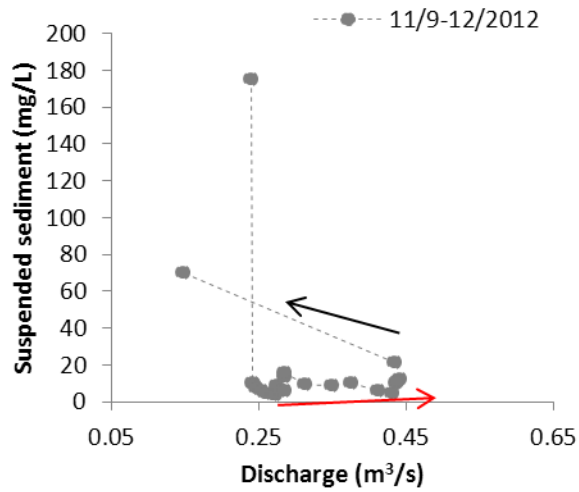

Money Creek - Event 7	11/9-12/2013	Units
Average TSS per storm	21.8	mg/L
Average Storm DISCHARGE	0.31	m^3/s
	10.61	ft^3/s
Peak Q	0.472	m^3/s
	16.662	ft^3/s
Total Load per storm/time step	34	kg
Average sediment Flux	110.86	mg/s
Hysteresis pattern	counter-clockwise	

EVENT 8

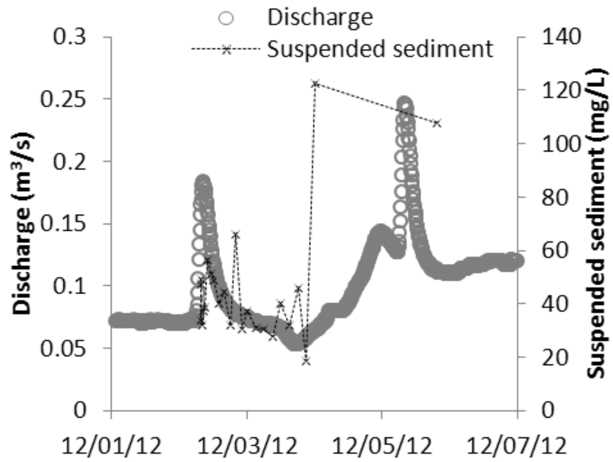

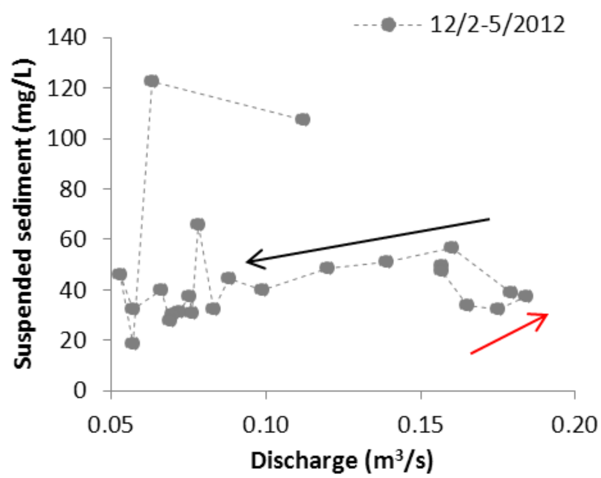

Money Creek - Event 8	12/2-6/2013	Units
Average TSS per storm	45.9	mg/L
Average Storm DISCHARGE	0.11	m^3/s
	3.76	ft^3/s
Peak Q	0.186	m^3/s
	6.566	ft^3/s
Total Load per storm/time step	8	kg
Average sediment Flux	26.87	mg/s
Hysteresis pattern	counter-clockwise	

EVENT 11

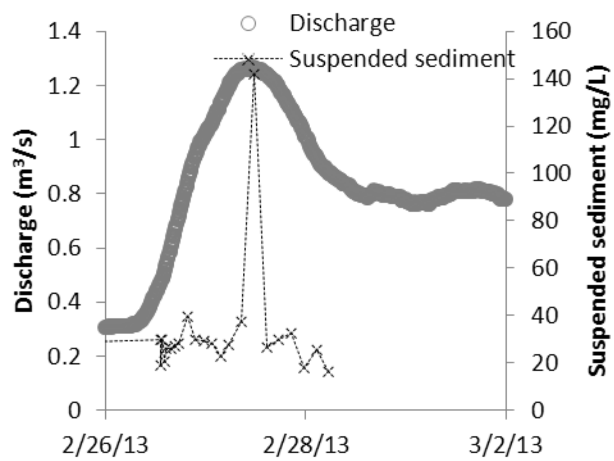

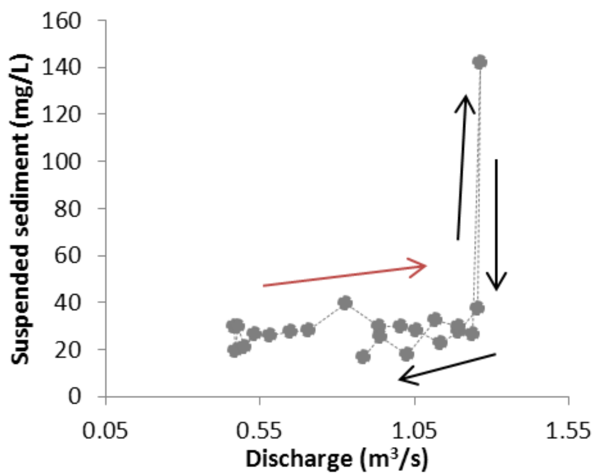

Money Creek - Event 11	2/26-28/2014	Units
Average TSS per storm	37.3	mg/L
Average Storm DISCHARGE	0.88	m^3/s
	31.20	ft^3/s
Peak Q	1.255	m^3/s
	44.302	ft^3/s
Total Load per storm/time step	96	kg
Average sediment Flux	661.11	mg/s
Hysteresis pattern	no pattern	